Lattice calculation of the zero-recoil form factor of $\bar{B}\to D^* l\bar{\nu}$: Toward a model independent determination of $|V_{cb}|$

Shoji Hashimoto,[1] Andreas S. Kronfeld,[2] Paul B. Mackenzie,[2] Sinéad M. Ryan,[3] and James N. Simone[2]
[1]*High Energy Accelerator Research Organization (KEK), Tsukuba 305-0801, Japan*
[2]*Fermi National Accelerator Laboratory, Batavia, Illinois 60510*
[3]*School of Mathematics, Trinity College, Dublin 2, Ireland*
(Received 30 October 2001; published 29 July 2002)

We develop a new method in lattice QCD to calculate the form factor $\mathcal{F}_{B\to D^*}(1)$ at zero recoil. This is the main theoretical ingredient needed to determine $|V_{cb}|$ from the exclusive decay $\bar{B}\to D^* l\bar{\nu}$. We introduce three ratios, in which most of statistical and systematic error cancels, making a precise calculation possible. We fit the heavy-quark mass dependence directly, and extract the $1/m_Q^2$ and three of the four $1/m_Q^3$ corrections in the heavy-quark expansion. In this paper we show how the method works in the quenched approximation, obtaining $\mathcal{F}_{B\to D^*}(1)=0.913^{+0.024}_{-0.017}\pm 0.016^{+0.003+0.000+0.006}_{-0.014-0.016-0.014}$ where the uncertainties come, respectively, from statistics and fitting, matching lattice gauge theory to QCD, lattice spacing dependence, light quark mass effects, and the quenched approximation. We also discuss how to reduce these uncertainties and, thus, to obtain a model-independent determination of $|V_{cb}|$.

DOI: 10.1103/PhysRevD.66.014503 PACS number(s): 12.38.Gc, 12.15.Hh, 13.20.He

I. INTRODUCTION

In flavor physics the Cabibbo-Kobayashi-Maskawa (CKM) matrix element V_{cb} plays an important role. Much of the phenomenology of *CP* violation centers around the unitarity triangle, and a precise value of $|V_{cb}|$ is needed to locate the triangle's apex in the complex plane. As a fundamental parameter of the standard model, V_{cb} sometimes appears in unexpected places. For example, the standard model prediction of the $K^0-\bar{K}^0$ mixing parameter ϵ_K is very sensitive to $|V_{cb}|$ [1].

The determination of $|V_{cb}|$ is made through inclusive and exclusive semileptonic *B* decays, but at present both methods are limited by theoretical uncertainties. The inclusive method requires a reliable calculation of the total semileptonic decay rate of the *B* meson, which can be done using the heavy quark expansion [2,3]. Ultimately this method is limited by the breakdown of local quark-hadron duality, which is difficult to estimate. The exclusive method, on the other hand, requires a theoretical calculation of the form factor $\mathcal{F}_{B\to D^*}$ of $\bar{B}\to D^* l\bar{\nu}$ decay. In this paper we take a step towards reducing the uncertainty in the exclusive method, by devising a precise method to compute the form factor at zero recoil in lattice QCD.

The differential rate for the semileptonic decay $\bar{B}\to D^* l\bar{\nu}_l$ is given by

$$\frac{d\Gamma}{dw}=\frac{G_F^2}{4\pi^3}m_{D^*}^3(m_B-m_{D^*})^2\sqrt{w^2-1}\,\mathcal{G}(w)|V_{cb}|^2\times|\mathcal{F}_{B\to D^*}(w)|^2, \tag{1.1}$$

where $w=v'\cdot v$ is the velocity transfer from the initial state (with velocity v) to the final state (with velocity v'). The velocity transfer is related to the momentum q transferred to the leptons by $q^2=m_B^2-2wm_Bm_{D^*}+m_{D^*}^2$, and it lies in the range $1\leqslant w<(m_B^2+m_{D^*}^2)/2m_Bm_{D^*}$. The function

$$\mathcal{G}(w)=\frac{w+1}{12}\left(5w+1+\frac{8w(w-1)m_Bm_{D^*}}{(m_B-m_{D^*})^2}\right) \tag{1.2}$$

has a kinematic origin, with $\mathcal{G}(1)=1$. Thus, given the form factor $\mathcal{F}_{B\to D^*}(w)$, one can use the measured decay rate to determine $|V_{cb}|$.

One makes use of the zero-recoil point $w=1$, even though the phase-space factor $\sqrt{w^2-1}$ suppresses the event rate, because then theoretical uncertainties are under better control. For $w>1$, $\mathcal{F}_{B\to D^*}(w)$ is a linear combination of several form factors of $\bar{B}\to D^*$ transitions mediated by the vector and axial vector currents. At zero recoil, however,

$$\mathcal{F}_{B\to D^*}(1)=h_{A_1}(1), \tag{1.3}$$

where h_{A_1} is a form factor of the axial vector current $\mathcal{A}^\mu$: namely,

$$\langle D^*(v)|\mathcal{A}^\mu|\bar{B}(v)\rangle=i\sqrt{2m_B2m_{D^*}}\epsilon'^\mu h_{A_1}(1). \tag{1.4}$$

More importantly, heavy-quark symmetry plays an essential role in constraining $h_{A_1}(1)$, leading to the simple heavy quark expansion [4,5]

$$h_{A_1}(1)=\eta_A\left[1-\frac{l_V}{(2m_c)^2}+\frac{2l_A}{2m_c2m_b}-\frac{l_P}{(2m_b)^2}\right], \tag{1.5}$$

including all terms of order $1/m_Q^2$. In Eq. (1.5), η_A is a short-distance radiative correction, which is known at the two-loop level [6,7], and the ls are long-distance matrix elements of the heavy-quark effective theory (HQET).[1] Heavy-quark symmetry normalizes the leading term inside the bracket to

[1]In the HQET literature, the ls are often called "hadronic parameters," because they are viewed as incalculable. In a QCD context, however, the are not free parameters, but calculable matrix elements.

unity [8] and, moreover, forbids terms of order $1/m_Q$ [9]. The $1/m_Q^2$ corrections are formally small—$(\bar{\Lambda}/2m_c)^2 \sim 4\%$—but one would like to reach better precision on $|V_{cb}|$, so these terms cannot be neglected.

There have been mainly two different methods used to estimate the $1/m_Q^2$ terms in Eq. (1.5), but neither has achieved a model independent calculation. One involves using a quark model [4,10] to estimate the ls. The other employs the zero-recoil sum rule [11]. Although based on a rigorous upper bound [12], to make a prediction of $\mathcal{F}_{B\to D^*}(1)$ this approach requires an assumption on the effects of higher excited states in the sum rule. Thus—just as with quark models—it is difficult to estimate, let alone reduce, the uncertainty associated with the estimate.

In this paper we take a step towards reducing the theoretical uncertainty by using lattice QCD to calculate $h_{A_1}(1) = \mathcal{F}_{B\to D^*}(1)$. Lattice QCD is, in principle, model independent, although here we work in the quenched approximation. The quenched approximation is not less rigorous than the methods used in Refs. [10,11]. From our point of view, however, the main advantage of the quenched approximation is that it allows us to learn how to control and estimate all other lattice uncertainties. With a proven technique, it is conceptually straightforward, if computationally demanding, to carry out a calculation in full QCD.

Until now three obstacles prevented even quenched lattice calculations of $h_{A_1}(1)$ to the needed precision. First, a direct Monte Carlo calculation of the matrix element in Eq. (1.4) suffers from a statistical error that is too large to be interesting. Second, the normalization of the lattice axial vector current was uncertain, being limited by a poorly converging perturbation series. Finally, early works [13] used *ad hoc* methods for heavy quarks on the lattice, which entailed a poorly controlled extrapolation in the heavy quark mass. We have devised methods to circumvent all three obstacles. The first two are handled with certain double ratios of correlation functions, in which the bulk of statistical and systematic uncertainties cancel [14]. The third obstacle—the problem of heavy-quark lattice artifacts—is overcome by using a systematic method for treating heavy quarks on the lattice, based on Wilson fermions [15]. This obstacle could also be overcome using lattice nonrelativistic QCD (NRQCD) [16], as in the work of Hein *et al.* [17].

In our work [14] on the form factor $h_+(1)$ in the decay $\bar{B}\to D l \bar{\nu}$ at zero recoil, a central role was played by the double ratio of matrix elements

$$\mathcal{R}_+ = \frac{\langle D|\bar{c}\gamma^4 b|\bar{B}\rangle\langle \bar{B}|\bar{b}\gamma^4 c|D\rangle}{\langle D|\bar{c}\gamma^4 c|D\rangle\langle \bar{B}|\bar{b}\gamma^4 b|\bar{B}\rangle} = |h_+(1)|^2, \qquad (1.6)$$

where

$$\langle D(v)|\mathcal{V}^\mu|\bar{B}(v)\rangle = i\sqrt{2m_B 2m_D}\, v^\mu h_+(1). \qquad (1.7)$$

In Ref. [14] we studied the heavy-quark mass dependence of $h_+(1)$, using a fit to obtain the $1/m_Q^2$ and $1/m_Q^3$ corrections. In this work we employ this double ratio and two similar ones. The first additional double ratio is

$$\mathcal{R}_1 = \frac{\langle D^*|\bar{c}\gamma^4 b|\bar{B}^*\rangle\langle \bar{B}^*|\bar{b}\gamma^4 c|D^*\rangle}{\langle D^*|\bar{c}\gamma^4 c|D^*\rangle\langle \bar{B}^*|\bar{b}\gamma^4 b|\bar{B}^*\rangle} = |h_1(1)|^2, \quad (1.8)$$

where the pseudoscalar mesons $\bar{B}$ and D, and their form factor $h_+(1)$, are replaced with the vector mesons $\bar{B}^*$ and D^*, and their form factor $h_1(1)$:

$$\langle D^*(v)|\mathcal{V}^\mu|\bar{B}^*(v)\rangle = i\sqrt{2m_{B^*}2m_{D^*}}\,\bar{\epsilon}'\cdot\epsilon v^\mu h_1(1). \qquad (1.9)$$

The second additional double ratio is

$$\mathcal{R}_{A_1} = \frac{\langle D^*|\bar{c}\gamma_j\gamma_5 b|\bar{B}\rangle\langle \bar{B}^*|\bar{b}\gamma_j\gamma_5 c|D\rangle}{\langle D^*|\bar{c}\gamma_j\gamma_5 c|D\rangle\langle \bar{B}^*|\bar{b}\gamma_j\gamma_5 b|\bar{B}\rangle} = \frac{h_{A_1}^{\bar{B}\to D^*}(1)h_{A_1}^{D\to \bar{B}^*}(1)}{h_{A_1}^{D\to D^*}(1)h_{A_1}^{\bar{B}\to \bar{B}^*}(1)} \equiv |\check{h}_{A_1}(1)|^2, \qquad (1.10)$$

where the axial vector current mediates pseudoscalar-to-vector transitions, leading to a double ratio of the form factor h_{A_1}. As stressed in Ref. [14], the double ratios overcome two of the obstacles in the lattice calculation, because numerator and denominator are so similar. Statistical fluctuations in the numerator and denominator are very highly correlated and largely cancel in the ratio. Also, most of the normalization uncertainty in the lattice currents cancels, leaving only a residual normalization factor that can be computed reliably in perturbation theory [18]. Indeed, all uncertainties scale as $\mathcal{R}-1$, rather than as $\mathcal{R}$.

Note that the double ratio $\mathcal{R}_{A_1}$ does not yield the desired form factor $h_{A_1}^{\bar{B}\to D^*}$, but instead the combination $\check{h}_{A_1}$, which is itself a double ratio of form factors. One can, however, extract $h_{A_1}(1)$ from the three double ratios $\mathcal{R}_+$, $\mathcal{R}_1$, and $\mathcal{R}_{A_1}$, at least to the order in the heavy-quark expansion given in Eq. (1.5). This possibility follows from the heavy quark expansions for $h_+(1)$ and $h_1(1)$ [4,5],

$$h_+(1) = \eta_V\left[1 - l_P\left(\frac{1}{2m_c} - \frac{1}{2m_b}\right)^2\right], \qquad (1.11)$$

$$h_1(1) = \eta_V\left[1 - l_V\left(\frac{1}{2m_c} - \frac{1}{2m_b}\right)^2\right], \qquad (1.12)$$

and comparing to Eq. (1.5). In $h_+(1)$ and $h_1(1)$ the absence of terms of order $1/m_Q$ [9] is easily understood, because charge conservation requires $h_+(1)=h_1(1)=1$ when $m_c = m_b$, and because the matrix elements defining them are symmetric under the interchange $m_c \leftrightarrow m_b$. Similarly, the heavy-quark expansion of the form factor ratio $\check{h}_{A_1}(1)$, obtained from $\mathcal{R}_{A_1}$, is

$$\check{h}_{A_1}(1)=\check{\eta}_A\left[1-l_A\left(\frac{1}{2m_c}-\frac{1}{2m_b}\right)^2\right], \qquad (1.13)$$

which follows immediately from Eq. (1.5), defining $\check{\eta}_A^2 = \eta_{A^{cb}}\eta_{A^{bc}}/\eta_{A^{cc}}\eta_{A^{bb}}$. Hence, by varying the heavy quark masses in the lattice calculation of the double ratios $\mathcal{R}_+$, $\mathcal{R}_1$, and $\mathcal{R}_{A_1}$, one can extract l_P, l_V, and l_A, respectively. Then, $h_{A_1}(1)=\mathcal{F}_{B\to D^*}(1)$ can be reconstituted through Eq. (1.5).

A key to this method is that heavy-quark symmetry requires the quantities l_P and l_V to appear in Eq. (1.5), as well as in Eqs. (1.11) and (1.12) [4,5]. A simple argument explains why. For each form factor there are three possible terms at order $1/m_Q^2-1/m_c^2$, $1/m_b^2$, and $1/m_cm_b$—and each multiplies an HQET matrix element. For $h_+(1)$ and $h_1(1)$ the particular form of the expansions is restricted by the $b\leftrightarrow c$ interchange symmetry, so only one HQET matrix element can appear in each case: l_P for $h_+(1)$ and l_V for $h_1(1)$. Interchange symmetry does not apply to the $\overline{B}\to D^*$ transition, however, so three HQET matrix elements are needed in the expansion of $h_{A_1}(1)$, Eq. (1.5). Two of them, however, coincide with l_P and l_V. If one flips the spin of the charmed quark in the $\overline{B}\to D$ transition in Eq. (1.7), one obtains the $\overline{B}\to D^*$ transition in Eq. (1.4), and in the limit of infinite charmed quark mass the matrix elements are identical, by heavy-quark spin symmetry. Consequently, the $1/m_b^2$ term in Eq. (1.5) must be the same as that in Eq. (1.11), namely $l_P/(2m_b)^2$. The same logic applied to the b quark's spin, starting from the $\overline{B}^*\to D^*$ transition in Eq. (1.9), implies that the $1/m_c^2$ term in Eqs. (1.5) and (1.12) must be the same, namely $l_V/(2m_c)^2$.

At order $1/m_Q^3$ there are, in general, four terms for each form factor. In Sec. V we show how the same kind of reasoning can be used to extract three of the four terms from the $1/m_Q^3$ behavior of the three double ratios. Including these corrections not only reduces the systematic error of the heavy quark expansion, but also reduces our statistical error, because fitted values for the quadratic and cubic terms are correlated.

In the remainder of this paper we describe the details of our lattice calculation of $\mathcal{F}_{B\to D^*}(1)=h_{A_1}(1)$, as sketched above. Discretization effects are studied by repeating the analysis at three different lattice spacings. The dependence on the light quark mass is expected to be small, which we are able to verify. After a thorough investigation of systematic uncertainties, we obtain

$$\mathcal{F}_{B\to D^*}(1)=0.913^{+0.024}_{-0.017}\pm 0.016^{+0.003+0.000+0.006}_{-0.014-0.016-0.014}, \qquad (1.14)$$

where the uncertainties come, respectively, from statistics and fitting, matching lattice gauge theory and HQET to QCD, lattice spacing dependence, light quark mass effects, and the quenched approximation. A preliminary report of this calculation based on our coarsest lattice appeared in Ref. [19], reporting $\mathcal{F}_{B\to D^*}(1)=0.935\pm 0.022^{+0.023}_{-0.024}$. The change comes mostly from the results on two finer lattices, partly from some secondary changes in the analysis, and partly from the inclusion of some contributions of order $1/m_Q^3$. Clearly, these central values are indistinguishable within the error bars.

The paper is organized as follows. In Sec. II we discuss how to combine heavy-quark theory and lattice gauge theory to calculate the needed matrix elements; in particular, we review how we are able to extract the $1/m_Q^2$ corrections [20]. Section II is fairly general and much of it also applies to lattice NRQCD. Specific details of our numerical work are given in Sec. III, including input parameters and the basic outputs. The ''Fermilab'' method for heavy quarks [15] requires matching the short-distance behavior of lattice gauge theory to QCD, which is discussed in Sec. IV. Section V shows a key feature of our analysis, namely the direct fitting of the heavy-quark mass dependence to obtain the power corrections in Eq. (1.5). A detailed discussion of the systematic uncertainties is in Sec. VI. Our result, Eq. (1.14), is compared to other methods in Sec. VII. Section VIII contains some concluding remarks.

II. CONTINUUM AND LATTICE MATRIX ELEMENTS

In this section we discuss how to obtain continuum-QCD, heavy-quark observables from lattice gauge theory. Discretization effects of the heavy quarks are a special concern, so they are discussed in detail in this section. For the light spectator quark we use well-known methods, and we provide details in Sec. III.

Discretization effects of the heavy quarks can be controlled by matching the lattice theory to HQET [20]. This is possible whether one discretizes the NRQCD effective Lagrangian [16], or one employs the nonrelativistic interpretation of Wilson fermions [15]. In either case, on-shell lattice matrix elements can be described by a version of (continuum) HQET, with effective Lagrangian (in the rest frame)

$$\mathcal{L}_{\rm HQET}=m_1\overline{h}_v h_v+\frac{\overline{h}_v\mathbf{D}^2h_v}{2m_2}+\frac{\overline{h}_v i\mathbf{\Sigma}\cdot\mathbf{B}h_v}{2m_{\mathcal{B}}}+\cdots, \qquad (2.1)$$

where h_v is the heavy-quark field of HQET, and $\mathbf{B}$ is the chromomagnetic field. The ''masses'' m_1, m_2, and $m_{\mathcal{B}}$ are short-distance coefficients; they depend on the bare couplings of the lattice action, including the gauge coupling. Matrix elements are completely independent of m_1 [20], so the important coefficients are m_2 and $m_{\mathcal{B}}$. The lattice NRQCD action has bare parameters that correspond directly to m_2 and $m_{\mathcal{B}}$. With Wilson fermions one must use the Sheikholeslami-Wohlert (SW) action [21], and adjust m_0 and $c_{\rm SW}$ to tune m_2 and $m_{\mathcal{B}}$. In practice, we tune m_2 nonperturbatively, using the heavy-light and quarkonium spectra, and $m_{\mathcal{B}}$ with the estimate of tadpole-improved, tree-level perturbation theory [22]. There are also terms of order $1/m_Q^2$ in the effective Lagrangian $\mathcal{L}_{\rm HQET}$, but they do not influence the double ratios, as discussed further below.

In this paper we use lattice currents that are constructed as in Ref. [15]. (An analogous set of currents can be constructed

for lattice NRQCD [24].) We distinguish the lattice currents V^μ and A^μ from their continuum counterparts $\mathcal{V}^\mu$ and $\mathcal{A}^\mu$. We define

$$V^\mu = \sqrt{Z_{V^{cc}} Z_{V^{bb}}}\,\overline{\Psi}_c i\gamma^\mu \Psi_b, \tag{2.2}$$

$$A^\mu = \sqrt{Z_{V^{cc}} Z_{V^{bb}}}\,\overline{\Psi}_c i\gamma^\mu \gamma_5 \Psi_b, \tag{2.3}$$

where the rotated field [15]

$$\Psi_q = [1 + a d_1 \boldsymbol{\gamma}\cdot \mathbf{D}_{\rm lat}]\psi_q, \tag{2.4}$$

and ψ_q is the lattice quark field ($q=c,b$) in the SW action. Here $\mathbf{D}_{\rm lat}$ is the symmetric, nearest-neighbor, covariant difference operator. In Eqs. (2.2) and (2.3) the factors $Z_{V^{qq}}$, $q=c,b$, normalize the flavor-conserving vector currents. Because for massive quarks only Z_V can be computed nonperturbatively, we choose to put Z_V into the definition of the axial current A^μ. In the work reported in this paper, we do not need to compute the factor $\sqrt{Z_{V^{cc}} Z_{V^{bb}}}$, because it cancels in the double ratios.

Matching the current V^μ to HQET requires further short-distance coefficients:

$$V^\mu \doteq C_{V_\parallel}^{\rm lat} v^\mu \overline{c_v} b_v - \frac{B_{Vc}^{\rm lat} \overline{c_v} \not{\tilde{D}}_\perp i\gamma_\perp^\mu b_v}{2m_{3c}} - \frac{B_{Vb}^{\rm lat} \overline{c_v} i\gamma_\perp^\mu \not{D}_\perp b_v}{2m_{3b}} + \cdots, \tag{2.5}$$

$$A^\mu \doteq C_{A_\perp}^{\rm lat} \overline{c_v} i\gamma_\perp^\mu \gamma_5 b_v + \frac{B_{Ac}^{\rm lat} v^\mu \overline{c_v} \not{\tilde{D}}_\perp \gamma_5 b_v}{2m_{3c}} - \frac{B_{Ab}^{\rm lat} v^{gm} \overline{c_v} \gamma_5 \not{D}_\perp b_v}{2m_{3b}} + \cdots, \tag{2.6}$$

where the symbol $\doteq$ implies equality of matrix elements, and b_v and c_v are HQET fields for the bottom and charmed quarks. At the tree level the short-distance coefficients $C_{V_\parallel}^{\rm lat}$, $C_{A_\perp}^{\rm lat}$, and $B_{hJ}^{\rm lat}$ all equal one. The free parameter d_1 in Eq. (2.4) can be adjusted to tune $1/m_{3Q}$ to $1/m_Q$. In the present calculations, we adjust d_1 with the estimate of tadpole-improved, tree-level perturbation theory, as explained in Ref. [15]. Further dimension-four operators, whose coefficients vanish at the tree level, are omitted from the right-hand sides of Eqs. (2.5) and (2.6); they are listed in Ref. [18].

The description in Eqs. (2.5) and (2.6) is in complete analogy with that for the continuum currents; namely,

$$\mathcal{V}^\mu \doteq C_{V_\parallel} v^\mu \overline{c_v} b_v - \frac{B_{Vc} \overline{c_v} \not{\tilde{D}}_\perp i\gamma_\perp^\mu b_v}{2m_c} - \frac{B_{Vb} \overline{c_v} i\gamma_\perp^\mu \not{D}_\perp b_v}{2m_b} + \cdots, \tag{2.7}$$

$$\mathcal{A}^\mu \doteq C_{A_\perp} \overline{c_v} i\gamma_\perp^\mu \gamma_5 b_v + \frac{B_{Ac} v^\mu \overline{c_v} \not{\tilde{D}}_\perp \gamma_5 b_v}{2m_c} - \frac{B_{Ab} v^\mu \overline{c_v} \gamma_5 \not{D}_\perp b_v}{2m_b} + \cdots. \tag{2.8}$$

The radiative corrections to the short-distance coefficients in Eqs. (2.5) and (2.6) differ from those in Eqs. (2.7) and (2.8), because the lattice modifies the physics at short distances. On the other hand, the HQET operators are the same throughout.

There are also terms of order $1/m_Q^2$ in the effective currents on the right-hand sides of Eqs. (2.5)–(2.8), although for brevity they are not written out. The most important operators to be added to Eqs. (2.5) and (2.6) are

$$V_{(1,1)}^\mu = \frac{[1+O(g^2)]\overline{c_v} \not{\tilde{D}}_\perp v^\mu \not{D}_\perp b_v}{2m_{3c} 2m_{3b}}, \tag{2.9}$$

$$A_{(1,1)}^\mu = \frac{[1+O(g^2)]\overline{c_v} \not{\tilde{D}}_\perp i\gamma_\perp^\mu \gamma_5 \not{D}_\perp b_v}{2m_{3c} 2m_{3b}}. \tag{2.10}$$

The corresponding terms to be added to Eqs. (2.7) and (2.8) are the same, except that $2m_c 2m_b$ appears in the denominators. Thus, our lattice currents enjoy the correct normalization for the $1/m_c m_b$ term, as long as d_1 is adjusted so that $m_{3Q}=m_Q$, as above. The HQET description also has terms of order $1/m_c^2$ and $1/m_b^2$. They contribute to the individual matrix elements $\langle D^{(*)}|J^\mu|B^{(*)}\rangle$, but their contributions drop out of the double ratios, see below.

Since we aim for the $1/m_Q^2$ corrections to the double ratios we must, however, discuss in more detail how these contributions are incorporated, when the lattice action and currents are constructed and normalized along the lines given above. The HQET description of matrix elements reveals several sources of such contributions [4,5,20]: (1) double insertions of the $1/m_Q$ terms in the effective Lagrangian $\mathcal{L}_{\rm HQET}$; (2) single insertions of the $1/m_Q$ terms in the effective Lagrangian into matrix elements of the $1/m_Q$ terms in the effective HQET currents; (3) single insertions of genuine $1/m_Q^2$ terms in the effective Lagrangian; (4) matrix elements of genuine $1/m_Q^2$ terms in the effective HQET currents.

The first set of contributions is correctly normalized at the same level of accuracy as the $1/m_Q$ terms of the action. The second set makes no contribution to zero recoil matrix elements whatsoever [20]. The third set also makes no contribution at zero recoil, because the leading terms in Eqs. (2.5) and (2.6) are Noether currents of the heavy-quark symmetries and, as in the proof of Luke's theorem, first corrections to Noether currents vanish [25,20].

One is left with the last set, which *does* contribute to the matrix elements $\langle D^{(*)}|J^\mu|B^{(*)}\rangle$. The HQET matrix elements of all dimension-five currents can be reduced to λ_1 and λ_2, which appear in the heavy-quark expansion of the mass [4]. In the double ratios, however, the following cancellation takes place [20]:

$$\frac{[1-\lambda(X_b/m_b^2-1/m_c m_b+X_c/m_c^2)]^2}{[1-\lambda(2X_c-1)/m_c^2][1-\lambda(2X_b-1)/m_b^2]} = 1-\lambda\left(\frac{1}{m_c}-\frac{1}{m_b}\right)^2, \tag{2.11}$$

where λ is proportional to λ_1 or λ_2. We write $1/m_c m_b$ for the correctly normalized contributions of Eqs. (2.9) and (2.10), and X_Q/m_Q^2 for the other, incorrectly normalized operators. The incorrectly normalized contributions cancel in the double ratios. In practice, the ''correctly normalized'' terms are normalized only at the tree level, leaving us with uncertainties of order $\alpha_s(\bar{\Lambda}/m_Q)^2$. Along with their small statistical and normalization uncertainties, the absence of maladjusted $1/m^2$ contributions is the double ratios' most important trait.

Once one is content to neglect corrections of order $\alpha_s(\bar{\Lambda}/m_Q)^2$, it is easy to obtain the continuum normalization of the lattice currents. By comparing the heavy-quark expansions for V^μ and A^μ to those for $\mathcal{V}^\mu$ and $\mathcal{A}^\mu$, one sees that

$$\mathcal{V}^\mu_{cb} \doteq \rho_{V^{cb}} V^\mu_{cb}, \tag{2.12}$$

$$\mathcal{A}^\mu_{cb} \doteq \rho_{A^{cb}} A^\mu_{cb}, \tag{2.13}$$

apart from discretization effects discussed above. The ρ factors are

$$\rho_{V^{cb}} = C_{V_\parallel}/C^{\rm lat}_{V_\parallel}, \tag{2.14}$$

$$\rho_{A^{cb}} = C_{A_\perp}/C^{\rm lat}_{A_\perp}, \tag{2.15}$$

and they are known at the one-loop level [18].

The matrix elements are obtained from three-point correlation functions. For the zero-recoil $B\to D$, $B^*\to D^*$ and $B\to D^*$ transitions the three-point function are, respectively,

$$C^{B\to D}(t_f,t_s,t_i) = \sum_{\mathbf{x},\mathbf{y}} \langle 0|\mathcal{O}_D(\mathbf{x},t_f)\overline{\Psi}_c\gamma_4\Psi_b(\mathbf{y},t_s) \times \mathcal{O}^\dagger_B(\mathbf{0},t_i)|0\rangle, \tag{2.16}$$

$$C^{B^*\to D^*}(t_f,t_s,t_i) = \sum_{\mathbf{x},\mathbf{y}} \langle 0|\mathcal{O}_{D*}(\mathbf{x},t_f)\overline{\Psi}_c\gamma_4\Psi_b(\mathbf{y},t_s) \times \mathcal{O}^\dagger_{B*}(\mathbf{0},t_i)|0\rangle, \tag{2.17}$$

$$C^{B\to D^*}(t_f,t_s,t_i) = \sum_{\mathbf{x},\mathbf{y}} \langle 0|\mathcal{O}_{D*}(\mathbf{x},t_f)\overline{\Psi}_c\gamma_j\gamma_5\Psi_b(\mathbf{y},t_s) \times \mathcal{O}^\dagger_B(\mathbf{0},t_i)|0\rangle, \tag{2.18}$$

where $\mathcal{O}_{B(*)}$ and $\mathcal{O}_{D(*)}$ are interpolating operators for the $B^{(*)}$ and $D^{(*)}$ mesons. In $C^{B^*\to D^*}$ the spins of the vector mesons are parallel, and in $C^{B\to D^*}$ the spin of the D^* lies in the j direction. These correlation functions are calculated by a Monte Carlo method, as usual in lattice QCD. In the limit of large time separations, the correlation functions become

$$C^{B\to D}(t_f,t_s,t_i) = \mathcal{Z}_D^{1/2}\mathcal{Z}_B^{1/2}\frac{\langle D|\overline{\Psi}_c\gamma_4\Psi_b|B\rangle}{\sqrt{2m_D}\sqrt{2m_B}} \times e^{-m_B(t_s-t_i)}e^{-m_D(t_f-t_s)}+\cdots, \tag{2.19}$$

$$C^{B^*\to D^*}(t_f,t_s,t_i) = \mathcal{Z}_{D^*}^{1/2}\mathcal{Z}_{B^*}^{1/2}\frac{\langle D^*|\overline{\Psi}_c\gamma_4\Psi_b|B^*\rangle}{\sqrt{2m_{D^*}}\sqrt{2m_{B^*}}} \times e^{-m_{B^*}(t_s-t_i)}e^{-m_{D^*}(t_f-t_s)} +\cdots, \tag{2.20}$$

$$C^{B\to D^*}(t_f,t_s,t_i) = \mathcal{Z}_{D^*}^{1/2}\mathcal{Z}_B^{1/2}\frac{\langle D^*|\overline{\Psi}_c\gamma_j\gamma_5\Psi_b|B\rangle}{\sqrt{2m_{D^*}}\sqrt{2m_B}} \times e^{-m_B(t_s-t_i)}e^{-m_{D^*}(t_f-t_s)} +\cdots, \tag{2.21}$$

where $m_{B(*)}$ and $m_{D(*)}$ are the masses of the $B^{(*)}$ and $D^{(*)}$ mesons. The normalization factors $\sqrt{\mathcal{Z}_{H(*)}/2m_{H(*)}}$ are conventional; they cancel when forming the double ratios, so we do not need them. The correlation functions defined in Eqs. (2.16)–(2.18) are the only objects needed from the Monte Carlo. In practice we hold $t_i=0$ and $t_f=T/2$ fixed and vary t_s over the range for which the lowest-lying states dominate the correlation functions, as is needed for Eqs. (2.19)–(2.21) to hold. ($T=N_T a$ is the temporal length of the lattice.)

From the correlation functions we form the following double ratios:

$$R_+(t) = \frac{C^{B\to D}(0,t,T/2)C^{D\to B}(0,t,T/2)}{C^{D\to D}(0,t,T/2)C^{B\to B}(0,t,T/2)}, \tag{2.22}$$

$$R_1(t) = \frac{C^{B^*\to D^*}(0,t,T/2)C^{D^*\to B^*}(0,t,T/2)}{C^{D^*\to D^*}(0,t,T/2)C^{B^*\to B^*}(0,t,T/2)}, \tag{2.23}$$

$$R_{A_1}(t) = \frac{C^{B\to D^*}(0,t,T/2)C^{D\to B^*}(0,t,T/2)}{C^{D\to D^*}(0,t,T/2)C^{B\to B^*}(0,t,T/2)}. \tag{2.24}$$

Apart from renormalization factors, these ratios correspond to the continuum ratios $\mathcal{R}_+$, $\mathcal{R}_1$, and $\mathcal{R}_{A_1}$. In the window of time separations t and $T/2-t$ for which the lowest-lying states dominate, all convention-dependent normalization factors cancel in the double ratios, and the ratios reduce to

$$\rho_{V^{cb}}\sqrt{R_+} = \sqrt{\mathcal{R}_+} = h_+(1), \tag{2.25}$$

$$\rho_{V^{cb}}\sqrt{R_1} = \sqrt{\mathcal{R}_1} = h_1(1), \tag{2.26}$$

$$\check{\rho}_{A^{cb}}\sqrt{R_{A_1}} = \sqrt{\mathcal{R}_{A_1}} = \check{h}_{A_1}(1), \tag{2.27}$$

where $\check{\rho}^2_A = \rho_{A^{cb}}\rho_{A^{bc}}/\rho_{A^{cc}}\rho_{A^{bb}}$. In particular, note that the axial current double ratio does not yield $h_{A_1}(1)$ directly, but

TABLE I. Input parameters to the numerical lattice calculations, together with some elementary output parameters. Error bars on the outputs refer to the last digit(s).

Inputs			
$\beta=6/g_0^2$	6.1	5.9	5.7
Volume, $N_S^3\times N_T$	$24^3\times 48$	$16^3\times 32$	$12^3\times 24$
Configurations	200	350	300
$c_{\rm SW}$	1.46	1.50	1.57
κ_h, m_0 (GeV)	0.080, 7.90	0.077, 6.03	0.062, 6.16
	0.090, 5.82	0.088, 4.36	0.089, 2.87
	0.097, 4.62	0.099, 3.06	0.100, 2.03
	0.100, 4.16	0.110, 2.02	0.110, 1.42
	0.115, 2.21	0.121, 1.16	0.119, 0.96
	0.122, 1.46	0.126, 0.83	0.125, 0.69
	0.125, 1.16		
κ_q, m_0 (GeV)	0.1373, 0.092	0.1385, 0.088	0.1405, 0.093
	0.1379, 0.039	0.1388, 0.073	
		0.1391, 0.057	
t range	[9,15]	[6,10]	[4,8]
Elementary outputs			
$\kappa_{\rm crit}$	0.13847^{+4}_{-2}	0.14017^{+3}_{-1}	0.14327^{+5}_{-2}
$a^{-1}_{\rm 1P\text{-}1S}$ (GeV)	2.64^{+17}_{-13}	1.81^{+7}_{-6}	1.16^{+3}_{-3}
$a^{-1}_{f\pi}$ (GeV)	2.40^{+10}_{-12}	1.47^{+6}_{-6}	0.89^{+2}_{-2}
u_0	0.8816	0.8734	0.8608
$\alpha_V(3.40/a)$	0.14533	0.15938	0.18265

instead $\check{h}_{A_1}(1)$, defined in Eq. (1.10). Once we have computed the left-hand sides of Eqs. (2.25)–(2.27) for several combinations of the heavy quark masses, we can fit the mass dependence to the form predicted by the heavy-quark expansions, Eqs. (1.11)–(1.13).

To summarize this section, let us review the steps needed to obtain the physical form factor $\mathcal{F}_{B\to D*}(1)$: (1) compute the three-point correlation functions and thence the ratios R_+, R_1, R_{A_1}; (2) multiply $\sqrt{R}_+$ and $\sqrt{R}_1$ with ρ_V/η_V, and $\sqrt{R}_{A_1}$ with $\check{\rho}_A/\check{\eta}_A$, to obtain $h_+(1)/\eta_V$, $h_1(1)/\eta_V$, and $\check{h}_{A_1}(1)/\check{\eta}_A$; (3) fit $1-h/\eta$ [where h/η is $h_+(1)/\eta_V$, $h_1(1)/\eta_V$, or $\check{h}_{A_1}(1)/\check{\eta}_A$] to the heavy-quark mass dependence expected from Eqs. (1.11)–(1.13); (4) use the resulting l_V, l_A, and l_P (and associated $1/m_Q^3$ terms) to reconstitute $h_{A_1}(1)=\mathcal{F}_{B\to D*}(1)$ via (the $1/m_Q^3$ version of) Eq. (1.5).

As discussed above, with the lattice action, currents, and normalization conditions chosen above, we obtain $h_{A_1}(1)$ with uncertainties of order $\alpha_s(\overline{\Lambda}/2m_c)^2$ and $\overline{\Lambda}^3/(2m_Q)^3$ from matching, although the fitting procedure also yields estimates of three of the four $1/m_Q^3$ terms in $h_{A_1}(1)$, as discussed in Sec. V.

III. LATTICE CALCULATION

This work uses three ensembles of lattice gauge field configurations, which have been used in previous work on heavy-light decay constants [26,27], $B\to\pi l\nu$ and $D\to\pi l\nu$ semileptonic form factors [28], light-quark masses [29], and quarkonia [30]. The quark propagators are the same as in Ref. [27], but we now use 200 instead of 100 configurations on the finest lattice (with $\beta=6.1$). The input parameters for these fields are in Table I, together with some elementary output parameters.

The quark propagators are computed from the Sheikholeslami-Wohlert (SW) action [21], which includes a dimension-five interaction with coupling $c_{\rm SW}$, sometimes called the ''clover'' coupling. For the light spectator quark we use customary normalization conditions for massless quarks with the SW action, so $c_{\rm SW}$ is adjusted to reduce the leading lattice-spacing effect of Wilson fermions. In practice, we adjust $c_{\rm SW}$ to the value u_0^{-3} suggested by tadpole-improved, tree-level perturbation theory [22], and the so-called mean link u_0 is calculated from the plaquette. The leading light-quark cutoff effect is then of order $\alpha_s\Lambda a$, multiplied by a numerical coefficient that is known to be small. For the heavy quarks we adjust $c_{\rm SW}$ to the same value, but, as explained in Sec. II, one should think of this adjustment as tuning a coefficient in the HQET effective Lagrangian.

The hopping parameter κ is related to the bare quark mass. For the heavy quarks, κ_h is varied over a wide range encompassing charm and bottom. For the light spectator quark, the first row of κ_q in Table I corresponds to the strange quark. To test the dependence of the form factors on the light quark mass, we repeat the analysis for a few lighter spectator quarks. Table I also lists the tadpole-improved bare quark mass in GeV,

$$am_0 = \frac{1}{u_0}\left(\frac{1}{2\kappa} - \frac{1}{2\kappa_{\rm crit}}\right), \tag{3.1}$$

where the critical quark hopping parameter $\kappa_{\rm crit}$ makes the pion massless. Although this mass is just a bare mass, it shows that the heavy quarks are heavy, and the light quarks light.

The lattice spacing a plays a minor role in our analysis, because both the lattice perturbation theory and the fitting to the heavy-quark mass dependence can be carried out in lattice units. The physical scale enters only in adjusting the heavy-quark hopping parameters to the physical mass spectra, and in studying the dependence of $h_{A_1}(1)$ on a. Table I contains two estimates of the lattice spacing, from the spin-averaged $1P$-$1S$ splitting of charmonium, $\Delta m_{1P\text{-}1S}$, and from the pion decay constant f_π.

The renormalized strong coupling $\alpha_V(3.40/a)$ at scale $3.40/a$ is determined as in Ref. [22]. In Sec. IV the coupling is run to $\alpha_V(q^*)$, where q^* is the optimal scale according to the Brodsky-Lepage-Mackenzie (BLM) prescription [23,22]. Then $\alpha_V(q^*)$ is used to calculate the short-distance coefficients ρ_V/η_V and $\check{\rho}_A/\check{\eta}_A$, which are introduced in Eqs. (2.25)–(2.27), as well as the coefficient η_A.

The right-hand side of Eq. (2.19) is the first term in a series, with additional terms for each radial excitation [and similarly for Eqs. (2.20) and (2.21)]. We reduce contamination from excited states in two ways. First, we keep the three points of the three-point function well separated in (Euclidean) time. The initial-state meson creation operator is always at $t_i=0$ and the final-state meson annihilation operator at $t_f = N_T/2$. We then vary the time t_s of the current, to see when the lowest-lying states dominate. The second way to isolate the lowest-lying states is to choose creation operators $\mathcal{O}^\dagger_{B(*)}$ and annihilation operators $\mathcal{O}_{D(*)}$ to provide a large overlap with the desired state. This is done by smearing out the quark and antiquark with $1S$ and $2S$ Coulomb-gauge wave functions, as in Ref. [31].

Figure 1 shows the isolation of the ground state in the ratios $R_+(t)$, $R_1(t)$, and $R_{A_1}(t)$. In each of the three modes we find a long plateau. We fit to a constant and obtain a precision at the percent level. For each ensemble, we choose the same fit range for all mass combinations listed in Table I. In Fig. 1 the resulting central values and error envelopes are given by the solid and dotted lines, respectively. Different fit ranges lead to slightly different, though consistent, results; this variation is folded in with the statistical error. Statistical errors, including the full correlation matrix in all fits, are determined from 1000 bootstrap samples for each ensemble. The bootstrap procedure is repeated with the same sequence for all quark mass combinations, and in this way the fully correlated statistical errors are propagated through all stages of the analysis.

Figure 1 also demonstrates a clear distinction between the $\overline{B}^* \to D^*$ and the other two modes. Consequently, one can already see that l_V is definitely greater than l_P and l_A, as expected from Refs. [10–12]. This is an important observation, because the largest $1/m_Q^2$ correction to $h_{A_1}(1)$ is $l_V/(2m_c)^2$.

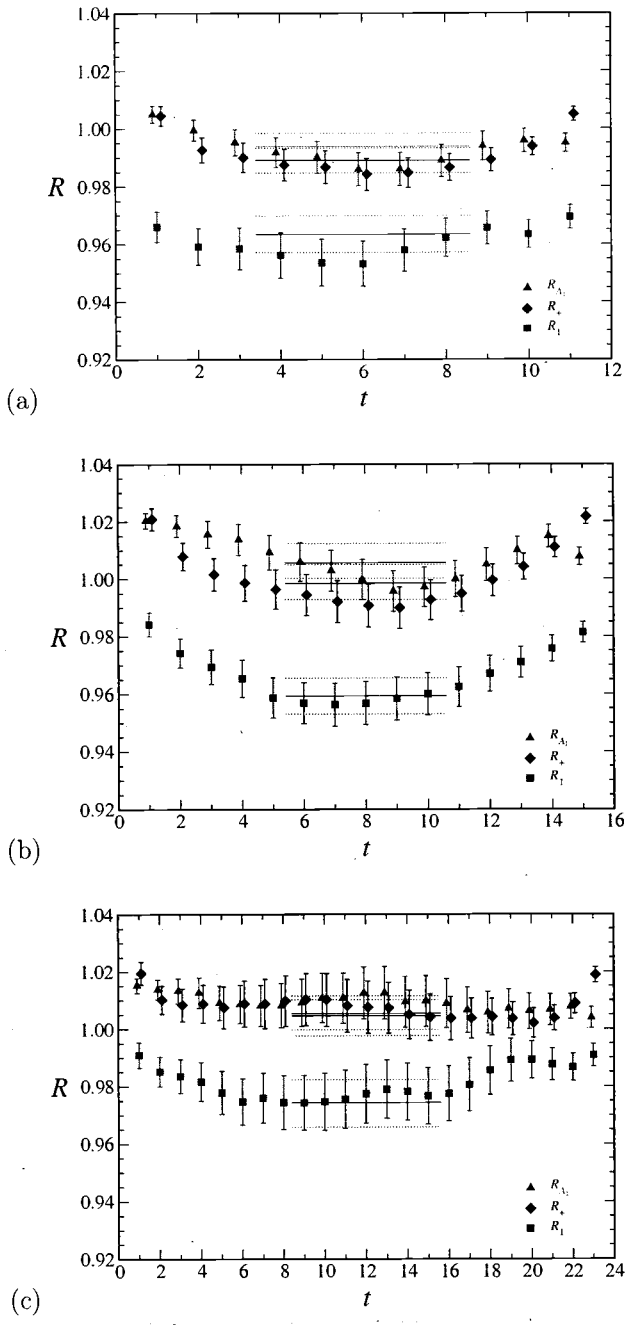

FIG. 1. Double ratios $R_{A_1}(t)$ (triangles), $R_+(t)$ (diamonds), and $R_1(t)$ (squares) at (a) $\beta=5.7$, (b) $\beta=5.9$, and (c) $\beta=6.1$. The heavy quark hopping parameters are (a) $(\kappa_b,\kappa_c)=(0.062,0.100)$, (b) $(\kappa_b,\kappa_c)=(0.088,0.121)$, and (c) $(\kappa_b,\kappa_c)=(0.097,0.122)$. The light quark mass is close to the strange quark mass. The lines represent constant fits in the indicated ranges.

IV. PERTURBATION THEORY

In this paper perturbation theory is needed to calculate the short-distance coefficients ρ_J $(J=V,A)$ defined in Eqs.

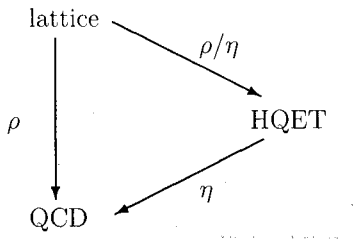

FIG. 2. Diagram illustrating how the matching factors ρ, η, and ρ/η match lattice gauge theory and HQET to QCD, and to each other.

(2.14) and (2.15), and η_J and $\check{\eta}_A$ appearing in Eqs. (1.5) and (1.11)–(1.13). The ρ factors match lattice gauge theory to QCD, and the η factors match HQET to QCD. To fit the heavy-quark mass dependence of the lattice double ratios, one must also match lattice gauge theory to HQET, and the corresponding factors are simply ρ_V/η_V and $\check{\rho}_A/\check{\eta}_A$. Figure 2 illustrates how these matching factors connect lattice gauge theory and HQET to QCD, and to each other.

Lattice perturbation theory often yields a series that appears to converge slowly. The two main causes of the poor convergence have been identified [22]: the bare gauge coupling is an especially poor expansion parameter, and when tadpole diagrams occur expansion coefficients are large. These two problems can be avoided by using a renormalized coupling as the expansion parameter and by using perturbation theory only for quantities in which tadpole diagrams largely cancel. Then lattice perturbation theory seems to converge as well as perturbation theory in continuum QCD.

To calculate the ρ factors only the vertex function is needed. By construction the self-energy contribution to wave-function renormalization, in particular the tadpole diagrams, cancels completely. Furthermore, even the vertex functions cancel partially, so the expansion coefficients should be small, as verified explicitly at the one-loop level [18]. Indeed, as $m_Q a \to 0$, $\rho \to 1$, and as $m_Q a \to \infty$, $\rho \to \eta$. Thus, despite the fact that only the one-loop correction to ρ_J is available [18], it seems likely that perturbation theory can be expected to behave well, especially when measured against other uncertainties in this calculation.

The other ingredient needed for an accurate perturbation series is a suitable renormalized coupling. We use the coupling α_V defined through the (Fourier transform of) the heavy quark potential, as suggested in Ref. [22]. The scale q^* of the running coupling $\alpha_V(q^*)$ is chosen according to the BLM prescription [23,22]:

$$\log(q^* a)^2 = \frac{{}^*\zeta^{[1]}}{\zeta^{[1]}}, \tag{4.1}$$

where ζ is ρ_V/η_V or $\check{\rho}_A/\check{\eta}_A$ when fitting the mass dependence of the double ratios, or η_A when reconstituting $h_{A_1}(1)$ with Eq. (1.5). The numerator ${}^*\zeta^{[1]}$ in Eq. (4.1) is obtained from the Feynman integrand for $\zeta^{[1]}$ by replacing the gluon propagator $D(k)$ by $\log(k^2a^2)D(k)$, where k is the gluon's momentum. Such terms arise at the higher-loop level, so the BLM prescription sums a class of higher-order corrections. Since in the cases at hand the one-loop integrals are ultraviolet and infrared finite, the only scales that can appear are $\sqrt{m_c m_b}$ and $1/a$. In general we find q^* to be a few GeV; the only exceptions occur when $(\rho_V/\eta_V)^{[1]}$ or $(\check{\rho}_A/\check{\eta}_A)^{[1]}$ are accidentally very small.

One of the advantages of the BLM prescription is that the scale depends on the renormalization scheme, in such a way that the value of the coupling itself does not depend on the scheme much. The coupling in an arbitrary scheme S is related to the V scheme by

$$\frac{(4\pi)^2}{g_S^2(q)} = \frac{(4\pi)^2}{g_V^2(q)} + \beta_0 b_S^{(1)} + b_S^{(0)} + O(g^2), \tag{4.2}$$

where for n_f light quarks $\beta_0 = 11 - 2n_f/3$, and $b_S^{(0)}$ is independent of n_f. In many cases, the β_0 term dominates; for example, for the $\overline{\rm MS}$ scheme, $b_{\overline{\rm MS}}^{(1)} = -5/3$ and $b_{\overline{\rm MS}}^{(0)} = -8$. If one chooses $q_S^* = q^* e^{-b_S^{(1)}/2}$, then $g_S^2(q_S^*)$ differs from $g_V^2(q^*)$ only by "non-BLM" terms of order $g^4(\beta_0 g^2)^{l-2}$, $l \geqslant 2$, which often are not very important.

In summary, we evaluate all short-distance coefficients with

$$\zeta = 1 + \alpha_V(q^*) 4\pi \zeta^{[1]} \tag{4.3}$$

and the appropriate BLM scale q^*. To check for the possible size of non-BLM two-loop corrections (which are unavailable for ρ_J), we also perform cross checks with $\alpha_{\overline{\rm MS}}(q^*_{\overline{\rm MS}})$. We obtain $\alpha_V(q^*)$ via two-loop running from [22]

$$\alpha_V(3.40/a) = \frac{2\alpha_{1\times 1}}{1 + \sqrt{1 - 4.74\alpha_{1\times 1}}}, \tag{4.4}$$

where $\alpha_{1\times 1} = -(3/\pi)\ln u_0 . u_0$ and $\alpha_V(3.40/a)$ are tabulated in Table I.

Table II contains the values of ρ_V/η_V and $\check{\rho}_A/\check{\eta}_A$ appropriate to the heavy quark mass combinations used in Sec. V. As expected, the perturbative corrections to these factors are small. The lattice coefficients $\rho_J^{[1]}$ and ${}^*\rho_J^{[1]}$ were obtained in Ref. [18]. The continuum coefficients are [32]

$$\eta_V^{[1]} = C_F 3 f(m_b/m_c)/16\pi^2, \tag{4.5}$$

$${}^*\eta_V^{[1]} = C_F 9 f(m_b/m_c)/32\pi^2 + \eta_V^{[1]} \ln(m_b a m_c a), \tag{4.6}$$

$$\check{\eta}_A^{[1]} = C_F 3 f(m_b/m_c)/16\pi^2, \tag{4.7}$$

$${}^*\check{\eta}_A^{[1]} = C_F 5 f(m_b/m_c)/32\pi^2 + \check{\eta}_A^{[1]} \ln(m_b a m_c a), \tag{4.8}$$

where

$$f(z) = \frac{z+1}{z-1}\ln z - 2. \tag{4.9}$$

TABLE II. Double ratios, computed in the Monte Carlo calculation, and (re)normalization factors, computed in perturbation theory to one-loop BLM order.

β, κ_q	(κ_b, κ_c)	$\sqrt{R_+}$	$\sqrt{R_1}$	ρ_V/η_V	$\sqrt{R_{A_1}}$	$\check{\rho}_A/\check{\eta}_A$
6.1	(0.080, 0.115)	1.0010^{+72}_{-75}	0.9851^{+74}_{-77}	1.0021	1.0024^{+68}_{-76}	0.9940
0.1373	(0.080, 0.122)	1.0030^{+101}_{-102}	0.9742^{+106}_{-114}	1.0008	1.0043^{+089}_{-106}	0.9919
	(0.090, 0.100)	1.0001^{+06}_{-06}	0.9990^{+06}_{-06}	1.0002	1.0002^{+06}_{-06}	1.0000
	(0.090, 0.125)	1.0050^{+70}_{-67}	0.9757^{+81}_{-84}	0.9978	1.0051^{+68}_{-68}	0.9908
	(0.097, 0.115)	1.0007^{+18}_{-18}	0.9948^{+21}_{-21}	1.0003	1.0012^{+16}_{-17}	0.9985
	(0.097, 0.122)	1.0023^{+35}_{-35}	0.9871^{+41}_{-43}	0.9991	1.0027^{+34}_{-34}	0.9954
	(0.100, 0.125)	1.0039^{+38}_{-36}	0.9838^{+45}_{-47}	0.9973	1.0034^{+36}_{-36}	0.9933
5.9	(0.077, 0.110)	0.9981^{+34}_{-28}	0.9872^{+33}_{-29}	1.0030	1.0009^{+32}_{-27}	1.0001
0.1385	(0.077, 0.121)	0.9971^{+58}_{-51}	0.9697^{+57}_{-54}	1.0035	1.0030^{+57}_{-50}	0.9770
	(0.077, 0.126)	0.9984^{+69}_{-67}	0.9549^{+69}_{-71}	1.0015	1.0054^{+70}_{-62}	0.9868
	(0.088, 0.110)	0.9993^{+15}_{-12}	0.9934^{+15}_{-13}	1.0013	1.0007^{+14}_{-12}	0.9999
	(0.088, 0.121)	0.9993^{+32}_{-29}	0.9795^{+32}_{-32}	1.0016	1.0028^{+33}_{-27}	0.9944
	(0.088, 0.126)	1.0011^{+46}_{-40}	0.9666^{+50}_{-47}	0.9995	1.0053^{+44}_{-38}	0.9903
	(0.099, 0.110)	0.9999^{+04}_{-03}	0.9980^{+04}_{-03}	1.0003	1.0003^{+04}_{-03}	0.9990
	(0.099, 0.121)	1.0003^{+16}_{-14}	0.9883^{+17}_{-16}	1.0000	1.0019^{+15}_{-13}	0.9969
	(0.099, 0.126)	1.0022^{+27}_{-23}	0.9780^{+31}_{-28}	0.9983	1.0041^{+25}_{-20}	0.9983
5.7	(0.062, 0.089)	0.9944^{+21}_{-26}	0.9923^{+26}_{-28}	1.0024	0.9975^{+23}_{-25}	1.0010
0.1405	(0.062, 0.100)	0.9895^{+42}_{-43}	0.9845^{+50}_{-52}	1.0050	0.9958^{+42}_{-48}	1.0017
	(0.062, 0.125)	0.9786^{+102}_{-118}	0.9339^{+122}_{-150}	1.0114	0.9888^{+121}_{-118}	1.0006
	(0.089, 0.100)	0.9992^{+03}_{-03}	0.9984^{+04}_{-04}	1.0005	0.9996^{+03}_{-03}	1.0001
	(0.089, 0.110)	0.9969^{+11}_{-10}	0.9929^{+15}_{-14}	1.0018	0.9985^{+11}_{-11}	1.0002
	(0.089, 0.119)	0.9945^{+21}_{-22}	0.9816^{+32}_{-32}	1.0035	0.9969^{+23}_{-24}	1.0000
	(0.089, 0.125)	0.9939^{+31}_{-34}	0.9673^{+50}_{-52}	1.0041	0.9958^{+34}_{-37}	1.0112
	(0.100, 0.125)	0.9979^{+15}_{-18}	0.9793^{+29}_{-29}	1.0022	0.9983^{+19}_{-21}	0.9958
	(0.110, 0.119)	0.9997^{+02}_{-02}	0.9972^{+04}_{-04}	1.0004	0.9998^{+02}_{-03}	0.9995

The important properties of $f(z)$ are $f(1)=0$, $f(1/z)=f(z)$. From the matching procedure derived in Ref. [18] one sees that the masses used in $f(m_b/m_c)$ should be the kinetic masses, namely the mass appearing in the kinetic term in Eq. (2.1).

Two different schemes for defining the kinetic quark mass are used in this paper, because they are simple to implement. Both employ the formula [15]

$$\frac{1}{am_2}=\frac{1}{e^{am_1}\sinh(am_1)}+\frac{1}{e^{am_1}}, \tag{4.10}$$

which is the tree-level relation between the kinetic mass m_2 and the rest mass m_1, for the SW action. One choice is to use the tree-level value for the rest mass $am_1=\log(1+am_0)$, with am_0 from Eq. (3.1), and we call the result the tree-level kinetic mass. The other is to use the one-loop rest mass in Eq. (4.10) [33], and we call the result the quasi-one-loop kinetic mass. (The kinetic mass receives further radiative corrections, but they are known to be small [33].) The second choice is essentially the (one-loop) perturbative pole mass. Although the difference between these schemes is formally of the non-BLM two-loop order, they could give slightly different results in practice. Thus, using both and comparing gives us a handle on the terms omitted from the perturbative series.

When reconstituting the physical form factor $h_{A_1}(1)$ with Eq. (1.5), one needs a numerical value for the short-distance coefficient η_A. Although it is known at the two-loop level [6,7], we use the one-loop, BLM results, so that all perturbation theory is treated on the same footing. Thus, we take [32]

$$\eta_A^{[1]}=C_F[3f(m_b/m_c)-2]/16\pi^2, \tag{4.11}$$

$$*\,\eta_A^{[1]}=C_F\left[\frac{5}{2}f(m_b/m_c)-1\right]/16\pi^2 + \eta_A^{[1]}\ln(m_b a m_c a). \tag{4.12}$$

For consistency, it is necessary to use the same definition of the quark mass in η_A as in ρ/η.

If we take the quasi-one-loop kinetic masses, which are very close to continuum pole masses, we find $z=m_{2c}/m_{2b}=\{0.308,0.296,0.290\}$, $q^*=\{2.94,3.08,3.12\}$ GeV, $\alpha_V(q^*)=\{0.205,0.203,0.208\}$ and, hence,

$$\eta_A=\{0.9713,0.9724,0.9724\} \tag{4.13}$$

for $\beta=\{5.7,5.9,6.1\}$, respectively. On the other hand, if we take the tree-level kinetic masses, we find $z=\{0.221,0.230,0.234\}$, $q^*=\{2.02,2.14,2.14\}$ GeV, $\alpha_V(q^*)=\{0.241,0.238,0.245\}$ and, hence,

$$\eta_A=\{0.9769,0.9758,0.9746\} \tag{4.14}$$

for $\beta=\{5.7,5.9,6.1\}$, respectively. Note that although the coupling is larger in this scheme (because the quark masses and, hence, q^* are smaller), the perturbative correction is smaller, because the magnitude of the coefficient $\eta_A^{[1]}$ decreases with z. As we shall see below, this scheme dependence in η_A is largely cancelled by the corresponding scheme dependence of the $1/m_Q^2$ corrections.

These values of η_A are slightly larger than the value 0.960 [6,7], which is widely adopted in the literature. The origin of this difference is the value used for α_s. We extract α_s from lattice QCD, which, in the quenched approximation, underestimates α_s slightly [30]. Also, there is nothing special about the standard value. It does not include uncertainties from the measured value of $\alpha_s(M_Z)$ or from the b and c masses. When our method is applied to full QCD, the double ratios, the gauge coupling, and the quark masses all can be determined self-consistently. In the meantime, we shall assign uncertainties from omitting the non-BLM two-loop term, adjusting the heavy quark masses, and the quenching effect on α_s.

V. HEAVY QUARK MASS DEPENDENCE

In this section we fit the (suitably normalized) double ratios to the form expected from the heavy quark expansion, yielding the quantities $a^2 l_V$, $a^2 l_A$, and $a^2 l_P$ (i.e., in lattice units). We find that it is also necessary and beneficial to incorporate terms of order $1/m_Q^3$ in the heavy quark expansion. The last step is then to combine these results into the main goal, which is $h_{A_1}(1)$.

Table II contains the results of our Monte Carlo calculations of $\sqrt{R_+}$, $\sqrt{R_1}$, and $\sqrt{R_{A_1}}$, in addition to the short-distance coefficients discussed in Sec. IV. This information is combined to form

$$\frac{\rho_V\sqrt{R_+}}{\eta_V}=\frac{h_+}{\eta_V}, \tag{5.1}$$

$$\frac{\rho_V\sqrt{R_1}}{\eta_V}=\frac{h_1}{\eta_V}, \tag{5.2}$$

$$\frac{\check{\rho}_A\sqrt{R_{A_1}}}{\check{\eta}_A}=\frac{\check{h}_{A_1}}{\check{\eta}_A}, \tag{5.3}$$

which we fit to the expected heavy-quark mass dependence. For each ratio in Eqs. (5.1)–(5.3) we try the fit

$$\frac{\rho\sqrt{R}}{\eta}=1-\frac{1}{4}\Delta_2^2\left(c^{(2)}+\frac{1}{2}c^{(3)}\Sigma_2\right), \tag{5.4}$$

where $c^{(2)}$ and $c^{(3)}$ are taken as free fit parameters, and

$$\Delta_2=\frac{1}{am_{2c}}-\frac{1}{am_{2b}}, \tag{5.5}$$

$$\Sigma_2=\frac{1}{am_{2c}}+\frac{1}{am_{2b}}. \tag{5.6}$$

In Eqs. (5.5) and (5.6), the subscript 2 indicates that the kinetic mass m_2 appears. For the quadratic term we use Δ_2^2, even though the masses m_2, $m_{\mathcal{B}}$, and m_3 all appear in the heavy-quark expansion to lattice QCD [20], because $m_2=m_{\mathcal{B}}=m_3$ at our level of accuracy. The rest mass m_1 in Eq. (2.1) drops out completely [20].

The $1/m_Q^3$ term is introduced in Eq. (5.4) to describe the data over a wide range of $1/m_Q$. The particular form $\Delta^2\Sigma$ is the only one that is invariant under the interchange symmetry $c\leftrightarrow b$ and vanishes for $m_c=m_b$. The $1/m_Q^3$ terms arise from many sources in HQET. Some of them, like triple insertions of the $1/m_Q$ terms in $\mathcal{L}_{\rm HQET}$, are correctly normalized with the choice of lattice action and currents made in Sec. III. They lead to $\Delta_2^2\Sigma_2$, with (to our accuracy) the kinetic mass everywhere. Others, like an insertion of a $1/m_Q^2$ term combined with an insertion of a $1/m_Q$ term, are not and would lead to $\Delta_2\Delta_X\Sigma_X$, where $\Delta_X\Sigma_X$ amounts to the difference of short-distance coefficients for the higher-dimension HQET operator $\mathcal{O}_X$.

The most important mismatches of $\Delta_X\Sigma_X$ are of order $\alpha_s am_{2c}$ and of order $(am_{2c})^2$, provided $am_{2c}<1$. They are not necessarily small but, perhaps, small enough to pin down the $1/m_Q^3$ corrections. The $1/m_Q^3$ contributions are influenced mostly by the region with large Σ, where $am_{2c}<0.6$. Thus, the fit coefficients $c^{(3)}$ can be expected to give a reasonable estimate of the desired $a^3 l^{(3)}$. Moreover, corrections of order $(\bar{\Lambda}/m_Q)^3$ are small to begin with, so even a large relative uncertainty in them leads to a small absolute uncertainty on $h_{A_1}(1)$.

As mentioned in the Introduction, there are four $1/m_Q^3$ terms in the heavy quark expansion of $h_{A_1}(1)$. If we write

$$h_{A_1}(1)=\eta_A[1+\delta_{1/m^2}+\delta_{1/m^3}], \tag{5.7}$$

then δ_{1/m^2} can be read off by comparing with Eq. (1.5), and

$$\delta_{1/m^3}=-\frac{l_V^{(3)}}{(2m_c)^3}+\frac{l_C^{(3)}}{(2m_c)^2(2m_b)}+\frac{l_B^{(3)}}{(2m_c)(2m_b)^2}-\frac{l_P^{(3)}}{(2m_b)^3}. \tag{5.8}$$

As suggested by the notation, $l_V^{(3)}$ is related to $h_1(1)$, and $l_P^{(3)}$ is related to $h_+(1)$. Repeating the argument based on heavy-quark spin symmetry, first for the b, then for the c, one sees that $h_{A_1}(1)$ and $h_1(1)$ share the term $l_V^{(3)}/(2m_c)^3$, and that $h_{A_1}(1)$ and $h_+(1)$ share the term $l_P^{(3)}/(2m_b)^3$, as given in Eq. (5.8). The other two terms in δ_{1/m^3} can be rewritten

$$\frac{l_C^{(3)}}{(2m_c)^2(2m_b)}+\frac{l_B^{(3)}}{(2m_c)(2m_b)^2}$$
$$=\frac{l_A^{(3)}}{(2m_c)(2m_b)}\left(\frac{1}{2m_c}+\frac{1}{2m_b}\right)$$
$$+\frac{l_D^{(3)}}{(2m_c)(2m_b)}\left(\frac{1}{2m_c}-\frac{1}{2m_b}\right), \tag{5.9}$$

where $l_A^{(3)}=[l_C^{(3)}+l_B^{(3)}]/2$ and $l_D^{(3)}=[l_C^{(3)}-l_B^{(3)}]/2$. Simple algebra shows that $l_A^{(3)}$ is indeed the coefficient of the $\Delta^2\Sigma$ term in the heavy-quark expansion of the ratio $\check{h}_{A_1}(1)$. Thus, to the extent that we can identify $c_{\{P,V,A\}}^{(3)}$ with $a^3 l_{\{P,V,A\}}^{(3)}$, we can reconstruct three of the four $1/m_Q^3$ corrections to $h_{A_1}(1)$. Only $l_D^{(3)}$ eludes us.

To show the quality of the fit to the mass dependence, we plot in Fig. 3 the quantity

$$Q=\frac{1-\rho\sqrt{R}/\eta}{\Delta_2^2}=\frac{1}{4}c^{(2)}+\frac{1}{8}c^{(3)}\Sigma_2 \tag{5.10}$$

vs $\Sigma_2=(1/am_{2c}+1/am_{2b})$, with the quasi-one-loop definition of am_2. Linear behavior in $(1/am_{2c}+1/am_{2b})$ is observed for each form factor, and we show the fit line in the figure. Some curvature is noticeable for the heaviest masses in Fig. 3(a), but the linear fit is still consistent within statistical errors. The growth of the statistical error toward the heavy-quark limit is a property of the heavy-light meson in the Monte Carlo calculation, and it is unavoidable [35,36].

The values of the fit parameters $c_{\{P,V,A\}}^{(2)}=a^2 l_{\{P,V,A\}}$ and $c_{\{P,V,A\}}^{(3)}$ are listed in Table III. In each case the extracted values of $c^{(2)}$ and $c^{(3)}$ are highly correlated. On the other hand, the combinations

$$a^2 l_V^{\rm eff}=c_V^{(2)}+\frac{c_V^{(3)}}{2am_{2c}}, \tag{5.11}$$

$$a^2 l_A^{\rm eff}=c_A^{(2)}+\frac{1}{2}c_A^{(3)}\left(\frac{1}{2am_{2c}}+\frac{1}{2am_{2b}}\right), \tag{5.12}$$

$$a^2 l_P^{\rm eff}=c_P^{(2)}+\frac{c_P^{(3)}}{2am_{2b}}, \tag{5.13}$$

are statistically more precise, because the correlated error cancels, for the first two especially so. These combinations appear directly in Eq. (5.7), provided we can reliably identify $c_V^{(3)}$ with $a^3 l_V^{(3)}$. We argued above that this identification is not too bad, because the coefficients $c^{(3)}$ should be influenced principally by smaller masses. As seen in Fig. 3, this predjudice is borne out, especially when the correlated statistics are taken into account: the best fits fit best for large $(1/am_{2c}+1/am_{2b})$.

The results presented in Fig. 3 and Table III are all for the quasi-one-loop definition of am_2. One should keep in mind

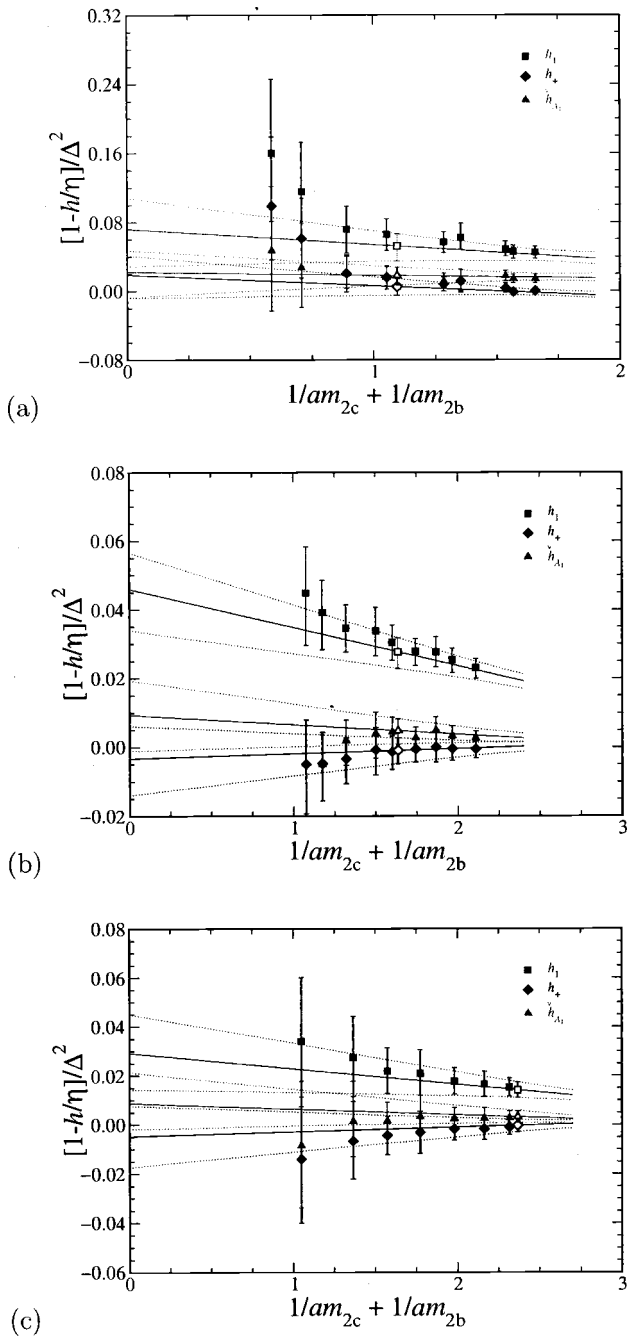

FIG. 3. $(1-h/\eta)/\Delta_2^2$ vs $1/am_{2c}+1/am_{2b}$ when h/η is $h_1(1)/\eta_V$ (squares), $h_+(1)/\eta_V$ (diamonds), and $\check{h}_{A_1}(1)/\check{\eta}_A$ (triangles) at (a) $\beta=5.7$, (b) $\beta=5.9$, and (c) $\beta=6.1$. Solid lines are best fits and dotted lines are error envelopes.

that the ls and $l^{(3)}$s have a well-defined interpretation as matrix elements within HQET. Their detailed definition depends on the renormalization scheme of operators in HQET, as discussed, for example, in Ref. [34]. After reconstituting $h_{A_1}(1)$, however, the scheme chosen should have only a minor, residual effect. Repeating the fits with the tree-level definition of $m_2 a$ changes the fit coefficients significantly (as expected). The change in $h_{A_1}(1)$ is, however, not great, and it is of order α_s/m_Q^2, as expected.

TABLE III. Coefficients in the $1/m_Q$ expansion, Eq. (5.4).

	h_+/η_V		h_1/η_V		$\check{h}_{A_1}/\check{\eta}_A$	
β	$c_P^{(2)}$	$c_P^{(3)}$	$c_V^{(2)}$	$c_V^{(3)}$	$c_A^{(2)}$	$c_A^{(3)}$
6.1	-0.019^{+051}_{-050}	0.015^{+035}_{-035}	0.117^{+063}_{-059}	-0.051^{+045}_{-041}	0.035^{+050}_{-042}	-0.018^{+035}_{-029}
5.9	-0.014^{+042}_{-038}	0.012^{+033}_{-030}	0.184^{+042}_{-048}	-0.089^{+032}_{-036}	0.037^{+040}_{-042}	-0.022^{+032}_{-034}
5.7	0.075^{+090}_{-108}	-0.100^{+099}_{-123}	0.289^{+144}_{-174}	-0.145^{+158}_{-186}	0.089^{+099}_{-118}	-0.030^{+111}_{-137}

To fix the physical values of m_b and m_c we compute the B_s and D_s spectra on the same ensembles of lattice gauge fields. Combining these inputs with the second row of Table III ($\beta=5.9$) (and omitting the $l_D^{(3)}$ contribution) we find

$$\delta_{1/m^n}=\delta_{1/m^2}+\delta_{1/m^3} \tag{5.14}$$

$$\simeq -\frac{l_V^{\rm eff}}{(2m_c)^2}+\frac{2l_A^{\rm eff}}{2m_c 2m_b}-\frac{l_P^{\rm eff}}{(2m_b)^2}$$

$$=-(0.0447^{+0.0078}_{-0.0070}), \tag{5.15}$$

which is needed in Eq. (5.7). The error quoted here is statistical only; systematic uncertainties are considered in detail in the next section. Equation (5.15) shows the power of our method: even with 15% statistical uncertainties on $\delta_{1/m^n}=h_{A_1}/\eta_A-1$, one can see that $h_{A_1}(1)$ itself can be very precise.

VI. SYSTEMATIC ERRORS

The intermediate result in Eq. (5.15) is obtained at one value of the lattice spacing, and with a spectator quark whose mass is close to that of the strange quark. In this section we consider the systematic uncertainty from varying a and m_q, as well as those from other sources. Table IV summarizes the results of this analysis, giving the absolute error on the main result, $h_{A_1}(1)$, and also fractional error on $1-h_{A_1}(1)$. As noted above, the uncertainties should scale with $1-h_{A_1}(1)$.

In the following subsections, we consider, in turn, the uncertainties arising from fitting Ansätze, which incorporate contamination in Eqs. (2.19)–(2.21) of excited states (Sec. VI A); heavy quark mass dependence (Sec. VI B); matching lattice gauge theory to HQET and QCD (Sec. VI C); lattice spacing dependence (Sec. VI D); light (spectator) quark mass dependence (Sec. VI E); and the quenched approximation (Sec. VI F). In Table IV the statistical uncertainty is added in quadrature to that from fitting, as discussed in Sec. VI A. As outlined in Sec. III, statistical uncertainties are computed with the bootstrap method and full covariance matrices.

A. Fitting and excited states

We define χ^2 in our fits with the full covariance matrix. For the plateau fits to $R(t)$

$$\chi^2=\sum_{t_1,t_2}[R(t_1)-R_{\rm fit}]\sigma^{-2}(t_1,t_2)[R(t_2)-R_{\rm fit}]. \tag{6.1}$$

Because the numerical data are so highly correlated, some components of the (inverse) matrix $\sigma^{-2}(t_1,t_2)$ cannot be determined well. These components are discarded, according to singular value decomposition (SVD), by eliminating eigenvectors of σ^2 whose eigenvalue $\lambda<r_{\rm SVD}\lambda_{\rm max}$, with $r_{\rm SVD}$ small. We find we have to set $r_{\rm SVD}\sim 10^{-2}$ to remove the noisy eigenvectors from χ^2 in Eq. (6.1).

A potential drawback of the double ratio technique is that an early plateau could be induced. We cope with this issue by trying many fit ranges for the time t_s of the current. In general, fits to a constant have good χ^2 and agree for fit ranges within the plateaus clearly seen in Fig. 1. For each ensemble

TABLE IV. Budget of statistical and systematic uncertainties for $h_{A_1}(1)$ and $1-h_{A_1}(1)$. The row labeled "total systematic" does not include uncertainty from fitting, which is lumped with the statistical error. The statistical error is that after chiral extrapolation.

Uncertainty	h_{A_1}			$1-h_{A_1}$ (%)		
statistics and fitting	$+0.0238$		-0.0173	$+27$		-20
adjusting m_c and m_b	$+0.0066$		-0.0068	$+8$		-8
α_s^2		± 0.0082			± 9	
$\alpha_s(\bar{\Lambda}/2m_Q)^2$		± 0.0114			± 13	
$(\bar{\Lambda})^3/(2m_Q)^3$		± 0.0017			± 2	
a dependence	$+0.0032$		-0.0141	$+4$		-16
chiral	$+0.0000$		-0.0163	$+0$		-19
quenching	$+0.0061$		-0.0143	$+7$		-16
total systematic	$+0.0171$		-0.0302	$+20$		-35
total (stat$\oplus$syst)	$+0.0293$		-0.0349	$+34$		-40

of lattice gauge fields we choose a single range for t_s for all three ratios and all heavy quark mass combinations. In each case, the range is chosen to give small statistical error on $R_{\rm fit}$, while maintaining a central value close to that from short intervals centered on $T/4$.

The expressions in Eqs. (2.19)–(2.21), relating three-point correlation functions to matrix elements, suppress terms from radial excitations of the desired, lowest-lying states. Because of heavy-quark symmetry, corresponding excitations of the D and B systems have similar wave functions and mass splittings. Consequently, their contribution to the double ratios largely cancels, leaving a residue that is suppressed by $(\overline{\Lambda}/m_Q)^2$ as well as the exponential factor for large times. Thus, the excited-state contamination in a double ratio scales as $R-1$, rather than R.

The fits of the heavy quark mass dependence are obtained by minimizing

$$\chi^2=\sum_{i,j}\left(Q_i-\frac{1}{4}c^{(2)}-\frac{1}{8}c^{(3)}\Sigma_{2i}\right)\sigma_{ij}^{-2}\left(Q_j-\frac{1}{4}c^{(2)}-\frac{1}{8}c^{(3)}\Sigma_{2j}\right), \tag{6.2}$$

where i,j label mass combinations. Once again, not all components of σ^{-2} are well determined. The fits are stable with $r_{\rm SVD}=\{5\times10^{-3},5\times10^{-4},1\times10^{-3}\}$ for $\beta=\{5.7,5.9,6.1\}$.

In summary, the fitting procedure to determine the double ratios R_+, R_1, and R_{A_1} depends on the fit range for t_s and on the cut $r_{\rm SVD}$ in the SVD. Similarly, the fit parameters of the heavy quark mass dependence, $c^{(2)}$ and $c^{(3)}$, depend on an additional SVD cut. The central values quoted here are from the fit ranges given in Table I, $r_{\rm SVD}=10^{-2}$ for $R(t)$, and $r_{\rm SVD}$ as given above for $c^{(2)}$ and $c^{(3)}$. We then repeat the analysis with larger and smaller SVD cuts and, for $R(t)$, with other fit ranges. The resulting variation in $h_{A_1}(1)$ is smaller than the statistical error of the ''best fits.'' Since excited states contribute differently in each fitting ansatz, the uncertainty in fitting $R(t)$ incorporates the uncertainty due to excited-state contamination. For convenience in analyzing the other systematics, the fitting error is added in quadrature to the statistical error.

B. Heavy quark mass dependence

The physical heavy quark masses enter when reconstituting h_{A_1} with Eq. (5.7). We determine them by tuning the hopping parameters κ_b and κ_c to reproduce the B_s and D_s spectra. To do so, we must compute the meson kinetic masses, which are somewhat noisy, and we must choose an observable to define the (inverse) lattice spacing. Thus, the tuned values of κ_b and κ_c have statistical uncertainties, from both the meson masses and from a^{-1}.

They also have systematic uncertainties. For example, the inverse lattice spacing a^{-1} is not the same when defined by the $1P$-$1S$ splitting of charmonium or by f_π, as noted in Table I. Similarly, κ_b and κ_c are not the same when quarkonium spectra are used instead of heavy-light spectra, although for κ_c this makes very little difference. In the end, we are left with a range for κ_b and κ_c and, hence, the heavy quark masses used in Eq. (5.7). This range leads to the error bar labeled ''adjusting m_b and m_c'' in Table IV.

C. Matching

As discussed in Sec. II our method for heavy quarks matches lattice gauge theory to QCD by normalizing the first few terms in the heavy-quark expansion [15,20]. This is necessary to keep heavy-quark discretization effects under control, but the approximate nature of the (perturbative) matching calculations leads to a series of uncertainties. The three most important of these are listed in Table IV.

The first is formally of order α_s^2. It comes from omitting the non-BLM radiative corrections to the factors ρ_J and η_J and from omitted loop corrections to the quark masses and to α_s. As discussed in Sec. IV, ρ_J comes from the cancellation of (continuum and lattice) vertex functions. Thus, by design, the coefficients of its perturbation series are small—usually smaller than those in η_J [18]. With η_A (and η_V) we can check explicitly how big the non-BLM two-loop corrections are. For example, the value of $h_{A_1}(1)$ is reduced by 0.0082 if we switch to the modified minimal subtraction ($\overline{\rm MS}$) scheme and include the non-BLM two-loop part of the η_J. Since the unknown two-loop corrections to the ρ_J could compensate, or even over-compensate, we take the two-loop uncertainty to be ±0.0082.

The next matching uncertainty is formally of order $\alpha_s(\overline{\Lambda}/2m_c)^2$, from tuning the lattice action and currents to HQET. Setting $\alpha_s=0.2$, $\overline{\Lambda}=500$ MeV, and $m_c=1.25$ GeV, one finds $\alpha_s(\overline{\Lambda}/2m_c)^2=0.008$. Another way to estimate this effect is to compare the analysis with tree-level heavy quark masses to the standard one with quasi-one-loop masses. The difference in $h_{A_1}(1)$ is in the same ballpark, at most $+0.0114$. Since other schemes for the quark mass could lead to shifts in the other direction, we take ±0.0114 as the uncertainty from this source.

The last matching uncertainty is of order $(\overline{\Lambda}/m_Q)^3$, from the omission of

$$\frac{l_D^{(3)}}{(2m_c)(2m_b)}\left(\frac{1}{2m_c}-\frac{1}{2m_b}\right)\sim0.0017, \tag{6.3}$$

assuming $l_D^{(3)}=\overline{\Lambda}^3$, $m_b=4$ GeV, and the same values as above. With same choices made above, we estimate that $l_A^{(3)}[1/(2m_c)+1/(2m_b)]/(2m_c2m_b)$ and $l_P^{(3)}/(2m_b)^3$ should be around 0.0033, and 0.0002, respectively. In Table V we show the actual effect of the included $1/m_Q^3$ corrections. The scatter of the different analyses bears out the latter estimates, lending credence to Eq. (6.3). Uncertainties in the included $1/m_Q^3$ terms are smaller than Eq. (6.3), because many of them are obtained correctly, and the mismatch in the others is small.

D. Lattice spacing dependence

The lattice calculation of h_{A_1} has lattice artifacts from heavy quarks, light quarks, and gluons. For the heavy quarks,

TABLE V. Scheme dependence of $h_{A_1}(1)$. For each value of β, the columns compare the scheme with tree-level and quasi-one-loop kinetic masses in η_J and in the mass dependence. The rows compare the effect of the $1/m^3$ contributions; here $\Sigma = 1/m_c + 1/m_b$ refers to the correction in Eq. (5.12). Each row includes the corrections from all preceding rows.

	$\beta = 6.1$		$\beta = 5.9$		$\beta = 5.7$	
l/m^n	tree	quasi	tree	quasi	tree	quasi
$1/m_Q^2$	$0.8755^{+0.0343}_{-0.0372}$	$0.8948^{+0.0416}_{-0.0430}$	$0.9078^{+0.0113}_{-0.0097}$	$0.9103^{+0.0140}_{-0.0130}$	$0.9365^{+0.0173}_{-0.0141}$	$0.9303^{+0.0275}_{-0.0234}$
$1/m_c^3$	$0.9331^{+0.0150}_{-0.0123}$	$0.9329^{+0.0205}_{-0.0167}$	$0.9362^{+0.0056}_{-0.0051}$	$0.9321^{+0.0082}_{-0.0072}$	$0.9549^{+0.0099}_{-0.0086}$	$0.9406^{+0.0162}_{-0.0151}$
$1/m_b^3$	$0.9332^{+0.0150}_{-0.0124}$	$0.9326^{+0.0206}_{-0.0166}$	$0.9363^{+0.0056}_{-0.0051}$	$0.9320^{+0.0082}_{-0.0073}$	$0.9551^{+0.0099}_{-0.0086}$	$0.9409^{+0.0163}_{-0.0151}$
$\Sigma/(m_c m_b)$	$0.9275^{+0.0126}_{-0.0114}$	$0.9274^{+0.0163}_{-0.0148}$	$0.9338^{+0.0057}_{-0.0052}$	$0.9300^{+0.0076}_{-0.0068}$	$0.9503^{+0.0097}_{-0.0079}$	$0.9400^{+0.0152}_{-0.0135}$

discretization effects and heavy-quark effects are inevitably intertwined [15,20], and are mostly part and parcel of the matching uncertainties considered above. The light quarks suffer from discretization effects of order $\alpha_s \Lambda a$ and $(\Lambda a)^2$; the gluons of order $(\Lambda a)^2$. That being said, we can test for the magnitude of discretization effects, by comparing the analysis of Sec. V for three lattice spacings. The results are plotted against a in Fig. 4, which also contains results for $h_+(1)$ and $h_1(1)$. The last two are much closer to 1 and their statistical uncertainties are correspondingly smaller. This underscores, once again, that the uncertainties scale as $1-h$.

The result for $h_{A_1}(1)$ with the available $1/m_Q^3$ contributions (solid triangles) is consistent with a constant. We take as our central value the average from the two finer lattices, because for them the (heavy-quark) discretization effects are smaller. This is

$$h_{A_1}(1) = 0.9293^{+0.0110}_{-0.0092}, \tag{6.4}$$

where the error is the statistical error on the average, with the error from fitting added in quadrature. In Fig. 4 the solid and dotted lines indicate this average and error band.

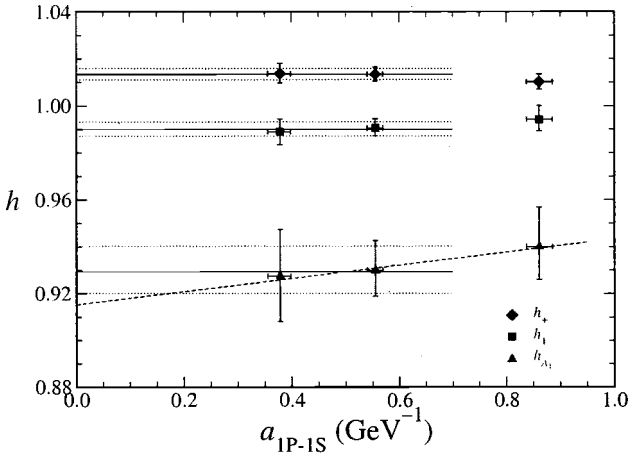

FIG. 4. Lattice spacing dependence of $h_{A_1}(1)$ (triangles), $h_+(1)$ (diamonds), and $h_1(1)$ (squares). The light quark mass is close to the strange quark mass. The solid (dotted) lines represent best fits (error envelopes).

The third point, at $a = 0.84$ GeV (from $\beta = 5.7$), has the greatest uncertainty from *heavy* quark discretization effects, so it is excluded from the central value. Instead we use it to estimate discretization uncertainties. If one assumes that discretization effects from the light spectator quark and gluons are negligible, then it would be appropriate to average all three. This average is slightly higher, and we take this increase as the upward systematic error bar. If, on the other hand, one assumes that the light spectator quark's discretization effects are responsible for the somewhat larger value of $h_{A_1}(1)$ on the coarsest lattice, then it would be appropriate to extrapolate linearly in a. The dashed line in Fig. 4 shows this extrapolation. The extrapolated value is significantly lower, and we take this decrease as the downward systematic error bar. The error bar resulting from these two estimates is very asymmetric: $^{+0.0032}_{-0.0141}$.

E. Chiral extrapolation

The calculations discussed so far have a spectator quark whose mass is near that of the strange quark. Figure 5 shows how $h_{A_1}(1)$ changes for lighter spectator quarks, on the lattice with $\beta = 5.9$, for which we have three values of the light quark mass. $h_{A_1}(1)$ is plotted against m_π^2 (in lattice units), which is a physical measure of the light quark mass. Since

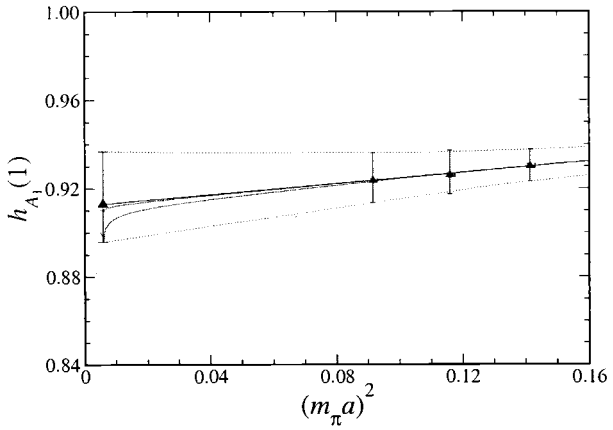

FIG. 5. Dependence of $h_{A_1}(1)$ at $\beta = 5.9$ on the mass of the light spectator quark. Here m_π^2 is the mass of the pseudoscalar meson consisting of two "light" quarks. The solid (dotted) lines represent the best linear fit (error envelope). The lower (upper) curves with a cusp add to the linear behavior the contribution in Eq. (6.6), taking $g_{D^*D\pi} = 0.60$ ($g_{D^*D\pi} = 0.27$).

the statistical errors in Fig. 5 are highly correlated, the downward trend in $h_{A_1}(1)$ is significant. The same trend is seen for $\beta=6.1$. Extrapolating linearly in m_π^2 to the physical pion, reduces the result in Eq. (6.4) to

$$h_{A_1}(1)=0.9130^{+0.0238}_{-0.0173} \tag{6.5}$$

and increases the statistical error. This value, using the average of the $\beta=5.9$ and 6.1 lattices and the chiral extrapolation from $\beta=5.9$, gives the central value in Eq. (1.14).

In the chiral expansion, the terms responsible for the linear behavior are formally of order $\overline{\Lambda}^2 m_\pi^2/(2m_c 4\pi f_\pi)^2$. Terms of order $\overline{\Lambda}^4/(2m_c 4\pi f_\pi)^2$ are larger for the physical pion mass, but are comparable for our artificially large pion masses. Randall and Wise [37] have computed the m_π^0 effect at one loop in chiral perturbation theory. They find

$$\frac{l_V(m_\pi)}{(2m_c)^2}=\frac{l_V(m_{\eta_s})}{(2m_c)^2}+\frac{g_{D^*D\pi}^2}{2}\left(\frac{\Delta^{(c)}}{4\pi f_\pi}\right)^2\left[\ln\frac{m_{\eta_s}^2}{m_\pi^2}+f(-x_\pi)-f(-x_{\eta_s})\right], \tag{6.6}$$

where $m_{\eta_s}^2=2m_K^2$ is the mass of the pseudoscalar meson with two strange quarks, $g_{D^*D\pi}$ is the D^*-D-π coupling, $\Delta^{(c)}=m_{D^*}-m_D=142$ MeV is the D^*-D mass splitting, and $x_a=\Delta^{(c)}/m_a$ $(a=\pi,\eta_s)$. For $g_{D^*D\pi}$ we consider the range 0.27–0.60, which encompasses estimates based on fits to experimental data ($g_{D^*D\pi}=0.27^{+0.06}_{-0.03}$ [38]), quark models ($g_{D^*D\pi}\approx 0.38$ [39]), quenched lattice QCD ($g_{D^*D\pi}=0.30\pm 0.16$ [40] or $g_{B^*B\pi}=0.42\pm 0.09$ [41]), and the recent measurement of the D^* width ($g_{D^*D\pi}=0.59\pm 0.07$ [42]).

The chiral loop function $f(x)$ has rather different behavior, depending on x. At $x=-1$, which turns out to be the physical region ($m_\pi\approx\Delta^{(c)}$), there is a cusp, and the value of f becomes large: $f(-1)\approx 11$ whereas $f(-x_{\eta_s})=f(-0.2)=0.53$. To illustrate this behavior, we have shown in Fig. 5 the sum of the second term in Eq. (6.6) and the linear fit. In the region where we have data, the term from Eq. (6.6) hardly varies, but near the physical limit, it bends the curve down. With the quoted range for $g_{D^*D\pi}$, the decrease in $h_{A_1}(1)$ amounts to 0.0033–0.0163, coming mostly in the region where $m_\pi\approx\Delta^{(c)}$, as shown in Fig. 5. In an unquenched calculation, one would add this contribution to $h_{A_1}(1)$. Because $g_{D^*D\pi}$ remains uncertain and because we are using the quenched approximation, we take it as an additional systematic uncertainty of $^{+0.0000}_{-0.0163}$. This effect and the amplification of the statistical error together make the chiral extrapolation the largest source of uncertainty.

F. Quenching

An important limitation of our numerical value for $h_{A_1}(1)$ is that the gauge fields were generated in the quenched approximation. The quenched approximation omits the back reaction of light quark loops on the gluons, and compensates the omission with a shift in the bare couplings. Two obvious consequences of quenching are that the coupling α_s runs incorrectly, and that pion loops [as in Eq. (6.6)] are not correctly generated.

Let us consider first the effect on the running coupling. The values for η_A in Sec. IV are obtained with the quenched coupling. If α_s is corrected for quenching, it is larger [30], and the short-distance coefficients are changed by -0.0050 for η_A and $+0.0032$ for η_V. These changes both reduce $h_{A_1}(1)$.

For the pion-loop contribution we can look to comparisons of quenched and unquenched calculations of other matrix elements. Studies of the decay constants f_B and f_D show discrepancies on the order of 10% between quenched and (partly) unquenched QCD [43,44]. A form factor, which is the overlap of two wave functions, is presumably less sensitive to quenching than a decay constant, which is a wave function at the origin. So, one should not expect the quenching error here to be more than 10%. Even in the quenched approximation all three double ratios tend to unity in the heavy-quark symmetry limit. Thus, the quenching error, like all others, scales with $R-1$, rather than R. We therefore apply the estimate of 10% to the long-distance part, δ_{1/m^n}, to obtain an error bar of ± 0.0061.

We estimate the total quenching uncertainty to be the sum of these two effects, or $^{+0.0061}_{-0.0143}$.

G. Summary

Combining Eq. (6.5) with the error budget in Table IV, we obtain

$$h_{A_1}(1)=0.9130^{+0.0238+0.0156+0.0032+0.0000+0.0061}_{-0.0173-0.0157-0.0141-0.0163-0.0143}, \tag{6.7}$$

where the error bars are from statistics and fitting, adjusting the heavy quark masses and matching, lattice spacing dependence, light quark mass dependence, and the quenched approximation. (The uncertainties on the second through fifth rows of Table IV are added in quadrature.) Adding all systematics in quadrature, we obtain

$$h_{A_1}(1)=\mathcal{F}_{B\to D^*}(1)=0.9130^{+0.0238+0.0171}_{-0.0173-0.0302}. \tag{6.8}$$

Although we have considered all sources of systematic uncertainty, it is not possible to disentangle them completely. For example, the lattice spacing dependence is not completely separated from the HQET matching uncertainties, and the quenched approximation affects the chiral behavior, the adjustment of m_c and m_b, and, through α_s, the matching coefficients.

VII. COMPARISON WITH OTHER METHODS

In this section we compare our method, based on lattice gauge theory, with others existing in the literature. To do so, it is convenient to refer to Eq. (1.5) and discuss how the short- and long-distance contributions are evaluated.

One approach, sometimes advertised as ''model-independent,'' is to estimate the ls with the nonrelativistic quark model [4,10]. The more recent estimate [10] takes

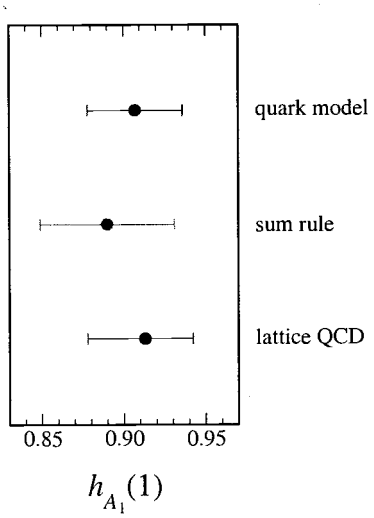

FIG. 6. Comparison of determinations of $h_{A_1}(1)=\mathcal{F}_{B\to D^*}(1)$ with nonperturbative input from the nonrelativistic quark model [10,6], a zero-recoil sum rule [46], and quenched lattice QCD.

δ_{1/m^2} to be -0.055 ± 0.025 by covering a range of ''all reasonable choices.'' Combining it with the two-loop calculation [6] of η_A, one obtains

$$\mathcal{F}_{B\to D^*}(1)=0.907\pm0.007\pm0.025\pm0.017, \qquad (7.1)$$

where the quoted uncertainties [10,6] are from perturbation theory, errors in the quark model estimate of the $1/m_Q^2$ terms, and the omission of $1/m_Q^3$ terms. Uncertainties from α_s and the quark masses are not included. A fair criticism of this approach is that it does not pay close attention to scheme dependence of the long- and short-distance contributions. The standard (μ-independent) result for η_A corresponds to renormalizing the operator insertions of HQET in the $\overline{\rm MS}$ scheme. The quark model estimates, on the other hand, are presumably in some other scheme, so there is a possibility to over- or undercount the contribution at the interface of long and short distances.

Another approach is based on a zero-recoil sum rule [11,3]. These authors prefer to introduce a concrete separation scale μ. In this scheme η_A and the ls depend explicitly on μ. The μ-dependent two-loop part of η_A is known [45]. A recent estimate of the zero-recoil form factor is [46]

$$\mathcal{F}_{B\to D^*}(1)=0.89\pm0.015\pm0.025\pm0.015\pm0.025, \qquad (7.2)$$

where the quoted uncertainties are from the unknown value of the kinetic energy $\mu_\pi^2(\mu)$, higher excitations with D^* quantum numbers and energy $E<m_{D^*}+\mu$, perturbation theory, and the omission of $1/m_Q^3$ terms. We note that both μ_π^2 and the excitation contribution should, in this scheme, cancel the $(\mu/m_Q)^2$ part of $\eta_A(\mu)$. Since there is no model-independent method to calculate the excitation contribution (except unquenched lattice QCD), it is not clear how to implement this cancellation.

As shown in Fig. 6, our result Eq. (1.14) agrees with the previous results, within errors, and the quoted errors are of comparable size. Our result includes an estimate of three of the four $1/m_Q^3$ contributions. All three are subject to a QED correction of $+0.007$ [47]. An important feature of our method is that, even in the quenched approximation, we are able to separate long- and short-distance contributions self-consistently. Indeed, we have repeated the calculation with two different schemes for the heavy quark masses, and the results are the same. Furthermore, it is clear that moving terms of order μ^2/m_Q^2 between the long- and short-distance parts will cancel out in our method, as long as it is done consistently. Finally, with future unquenched calculations in lattice QCD, our method allows for a systematic reduction in the theoretical error on $|V_{cb}|$.

VIII. CONCLUSIONS

We have developed a method to calculate the zero recoil form factor of $\overline{B}\to D^* l\nu$ decay. We introduce three double ratios in which the bulk of statistical and systematic errors cancels, thus enabling a precise calculation of $\mathcal{F}_{B\to D^*}(1)$. By matching lattice gauge theory to HQET, we are able to separate long-distance from short-distance contributions. Then the coefficients in the $1/m_Q$ expansion are obtained by fitting the numerical data. In this way we obtain the (leading) $1/m_Q^2$ corrections and three of the four $1/m_Q^3$ corrections. A similar approach has already been taken for $B\to Dl\nu$ [14].

Our result in the quenched approximation, $\mathcal{F}_{B\to D^*}(1)=0.913^{+0.024+0.017}_{-0.017-0.030}$, is consistent with results based on other ways of treating nonperturbative QCD. By using the quenched approximation we are able to gain control over all other uncertainties. Note, however, that the second error bar incorporates (among others) our estimate of the uncertainty from quenching. Furthermore, despite the shortcomings of the quenched approximation, it is not less rigorous than competing determinations of $\mathcal{F}_{B\to D^*}(1)$, which use either nonrelativistic quark models or a subjective estimate of the ''excitation contribution.'' With recent measurements of $|V_{cb}|\mathcal{F}_{B\to D^*}(1)$ from CLEO [48], the CERN e^+e^- collider LEP experiments [49], and Belle [50], our result implies

$$10^3|V_{cb}|=\begin{cases} 45.9\pm2.4^{+1.8}_{-1.4} & [48], \\ 38.7\pm1.8^{+1.5}_{-1.2} & [49], \\ 39.3\pm2.5^{+1.6}_{-1.2} & [50], \end{cases} \qquad (8.1)$$

where the second, asymmetric error comes from adding all our uncertainties in quadrature. Here we have included the QED correction to $\mathcal{F}_{B\to D^*}(1)$ of $+0.007$.

Since several groups have started partially unquenched lattice calculations of spectrum and decay constants, we conclude with some remarks on the prospects for $\mathcal{F}_{B\to D^*}(1)$. In this context, ''partially quenched'' means that the valence and sea quarks have different, and separately varied, masses. The analysis presented here shows that the double ratios bring the statistical precision under control, and that fitting the heavy-quark mass dependence is straightforward. Two of our larger systematic uncertainties will improve simply by including dynamical quarks. First, the self-consistent deter-

mination of the heavy-quark masses and of α_s will improve. At present, we believe the quenching bias in α_s, which affects the short-distance contribution, to be the largest source of uncertainty from the quenched approximation. Second, partially quenched numerical data are enough to extract the physical result, because one can use the recently derived result in partially quenched chiral perturbation theory [51].

The other two main sources of systematic uncertainty are the lattice spacing dependence and the matching of lattice gauge theory to HQET and QCD. The former is mostly a matter of computing. Indeed, our present estimate may be conservative, as it is driven by the coarsest lattice. To decrease the matching uncertainties, one must calculate the normalization factor to two loops and calculate the $1/m_Q^2$ corrections to one loop. The latter is not quite as hard as it might seem. Heavy-quark symmetry protects the needed matrix elements, so one only needs the one-loop calculation of the chromomagnetic term in the effective Lagrangian (a $1/m_Q$ term) and the $1/m_Q$ and mixed $1/m_c m_b$ terms in the currents. (An alternative to perturbation theory would be to develop a fully nonperturbative matching scheme for heavy quarks, including the $1/m_Q^n$ corrections.)

With the improvements from unquenched simulations, a more detailed study of lattice spacing dependence, and higher order matching calculations, it is conceivable that the error on $\mathcal{F}_{B\to D*}(1)$ could be brought to or below 1%. At this level, it would become crucial to compute, possibly by similar methods, the slope and curvature of $\mathcal{F}_{B\to D*}(w)$ near $w=1$. Then the determination of $|V_{cb}|$ would not only become very precise, but also truly model-independent.

ACKNOWLEDGMENTS

We thank Aida El-Khadra for helpful discussions. High-performance computing was carried out on ACPMAPS; we thank past and present members of Fermilab's Computing Division for designing, building, operating, and maintaining this supercomputer, thus making this work possible. Fermilab is operated by Universities Research Association Inc., under contract with the U.S. Department of Energy. S.H. is supported in part by the Grants-in-Aid of the Japanese Ministry of Education under Contract No. 11740162. A.S.K. would like to thank the Aspen Center for Physics for hospitality while writing part of this paper.

[1] J. L. Rosner, Nucl. Instrum. Methods Phys. Res. A **408**, 308 (1998).
[2] P. Ball, M. Beneke, and V. M. Braun, Phys. Rev. D **52**, 3929 (1995).
[3] I. Bigi, M. Shifman, and N. Uraltsev, Annu. Rev. Nucl. Part. Sci. **47**, 591 (1997).
[4] A. F. Falk and M. Neubert, Phys. Rev. D **47**, 2965 (1993).
[5] T. Mannel, Phys. Rev. D **50**, 428 (1994).
[6] A. Czarnecki, Phys. Rev. Lett. **76**, 4124 (1996).
[7] A. Czarnecki and K. Melnikov, Nucl. Phys. **B505**, 65 (1997).
[8] N. Isgur and M. B. Wise, Phys. Lett. B **232**, 113 (1989); **237**, 527 (1990).
[9] M. E. Luke, Phys. Lett. B **252**, 447 (1990).
[10] M. Neubert, Phys. Lett. B **338**, 84 (1994).
[11] M. Shifman, N. G. Uraltsev, and A. Vainshtein, Phys. Rev. D **51**, 2217 (1995); **52**, 3149(E) (1995).
[12] I. Bigi, M. Shifman, N. G. Uraltsev, and A. Vainshtein, Phys. Rev. D **52**, 196 (1995).
[13] UKQCD Collaboration, S. P. Booth *et al.*, Phys. Rev. Lett. **72**, 462 (1994); UKQCD Collaboration, N. Hazel, Nucl. Phys. B (Proc. Suppl.) **34**, 471 (1994).
[14] S. Hashimoto, A. X. El-Khadra, A. S. Kronfeld, P. B. Mackenzie, S. M. Ryan, and J. N. Simone, Phys. Rev. D **61**, 014502 (2000); Nucl. Phys. B (Proc. Suppl.) **73**, 399 (1999).
[15] A. X. El-Khadra, A. S. Kronfeld, and P. B. Mackenzie, Phys. Rev. D **55**, 3933 (1997).
[16] G. P. Lepage and B. A. Thacker, Nucl. Phys. B (Proc. Suppl.) **4**, 199 (1987); B. A. Thacker and G. P. Lepage, Phys. Rev. D **43**, 196 (1991); G. P. Lepage, L. Magnea, C. Nakhleh, U. Magnea, and K. Hornbostel, *ibid.* **46**, 4052 (1992).
[17] J. Hein, P. Boyle, C. T. H. Davies, J. Shigemitsu, and J. H. Sloan, Nucl. Phys. B (Proc. Suppl.) **83**, 298 (2000).
[18] A. S. Kronfeld and S. Hashimoto, Nucl. Phys. B (Proc. Suppl.) **73**, 387 (1999); J. Harada, S. Hashimoto, A. S. Kronfeld, and T. Onogi, Phys. Rev. D **65**, 094514 (2002).
[19] J. N. Simone *et al.*, Nucl. Phys. B (Proc. Suppl.) **83**, 334 (2000).
[20] A. S. Kronfeld, Phys. Rev. D **62**, 014505 (2000).
[21] B. Sheikholeslami and R. Wohlert, Nucl. Phys. **B259**, 572 (1985).
[22] G. P. Lepage and P. B. Mackenzie, Phys. Rev. D **48**, 2250 (1993).
[23] S. J. Brodsky, G. P. Lepage, and P. B. Mackenzie, Phys. Rev. D **28**, 228 (1983).
[24] UKQCD Collaboration, P. Boyle and C. Davies, Phys. Rev. D **62**, 074507 (2000).
[25] M. Ademollo and R. Gatto, Phys. Rev. Lett. **13**, 264 (1964).
[26] A. Duncan *et al.*, Phys. Rev. D **51**, 5101 (1995).
[27] A. X. El-Khadra *et al.*, Phys. Rev. D **58**, 014506 (1998).
[28] J. N. Simone *et al.*, Nucl. Phys. B (Proc. Suppl.) **73**, 393 (1999); A. X. El-Khadra *et al.*, Phys. Rev. D **64**, 014502 (2001).
[29] B. J. Gough *et al.*, Phys. Rev. Lett. **79**, 1622 (1997).
[30] A. X. El-Khadra, G. Hockney, A. S. Kronfeld, and P. B. Mackenzie, Phys. Rev. Lett. **69**, 729 (1992).
[31] A. Duncan, E. Eichten, and H. Thacker, Phys. Lett. B **303**, 109 (1993).
[32] M. Neubert, Phys. Lett. B **341**, 367 (1995).
[33] B. P. G. Mertens, A. S. Kronfeld, and A. X. El-Khadra, Phys. Rev. D **58**, 034505 (1998).
[34] A. S. Kronfeld and J. N. Simone, Phys. Lett. B **490**, 228 (2000).
[35] G. P. Lepage, Nucl. Phys. B (Proc. Suppl.) **26**, 45 (1992).
[36] S. Hashimoto, Phys. Rev. D **50**, 4639 (1994).
[37] L. Randall and M. B. Wise, Phys. Lett. B **303**, 135 (1993).
[38] I. W. Stewart, Nucl. Phys. **B529**, 62 (1998).

[39] R. Casalbuoni *et al.*, Phys. Rep. **281**, 145 (1997).
[40] JLQCD Collaboration, S. Aoki *et al.*, Phys. Rev. D **64**, 114505 (2001).
[41] UKQCD Collaboration, G. M. de Divitiis, L. Del Debbio, M. Di Pierro, J. M. Flynn, and C. Michael, Nucl. Phys. B (Proc. Suppl.) **83**, 277 (2000).
[42] CLEO Collaboration, A. Anastassov *et al.*, Phys. Rev. D **65**, 032003 (2002).
[43] C. Bernard *et al.*, Phys. Rev. Lett. **81**, 4812 (1998); Nucl. Phys. B (Proc. Suppl.) **83**, 289 (2000); **94**, 346 (2001).
[44] CP-PACS Collaboration, A. Ali Khan *et al.*, Phys. Rev. D **64**, 034505 (2001); **64**, 054504 (2001).
[45] A. Czarnecki, K. Melnikov, and N. Uraltsev, Phys. Rev. D **57**, 1769 (1998).
[46] N. Uraltsev, in *At the Frontier of Particle Physics: Handbook of QCD*, edited by M. Shifman (World Scientific, Singapore, 2001), hep-ph/0010328.
[47] *The BaBar Physics Book: Physics at an Asymmetric B Factory*, edited by P. F. Harrison and H. R. Quinn (BaBar Collaboration), SLAC-R-0504.
[48] CLEO Collaboration, K. Ecklund, talk at BCP4, Ise-Shima, Japan, 2001, http://www.ins.cornell.edu/public/TALK/2001/; CLEO Collaboration, R. Briere, talk at Heavy Flavors 9, Pasadena, CA, 2001, http://3w.hep.caltech.edu/HF9/
[49] LEP V_{cb} Working Group, http://lepvcb.web.cern.ch/LEPVCB/Winter.html
[50] Belle Collaboration, H. Kim, talk at Heavy Flavors 9, Pasadena, CA, 2001, http://3w.hep.caltech.edu/HF9/
[51] M. J. Savage, Phys. Rev. D **65**, 034014 (2002).